Chapter 2
Viscoelastic Contact/Impact Rheological Models

The first part of this chapter is dedicated to the analysis of viscoelastic and viscoelasto-plastic rheological contact models (linear and nonlinear parallel spring-dashpot assemblies). The linear spring-dashpot model is studied, and a detailed survey of nonlinear models (like Simon-Hunt-Crossley model and its many variations) as well as other types of assemblies with dry friction elements is made. Emphasis is put on the model's well-posedness, where complementarity systems may be used as a nice mathematical framework. The second part presents some well-posedness results (existence and uniqueness of solutions) of Lagrange dynamics with unilateral constraints and impacts, considering them as the limit of compliant systems when contact stiffness grows unbounded.

Bodies that collide possess a certain compliance and deform during an impact (locally around the contact point, and globally due to vibrations in the bodies). The collision duration is strictly positive.[1] Vibrations may even play in some cases a more important role than the local deformations. Consequently, rigid body dynamics may be considered as a limit case only, which however does not at all preclude its practical as well as theoretical utility. Moreover, the very short collision durations allow one to safely work with two time-scales in many practical cases. Historically, it has very often been difficult for certain scientists to accept the idea of perfect rigidity [1307]. For instance, Leibniz himself [721, 722] (and Bernoulli after him [134]) refused this idea because rigidity yields violation of the "law of continuity" in nature. A strong scientific debate motivated by the London Royal Society in 1668 also concerned the concept of "hardness" (which is to be understood as rigidity in this context): is a hard body able to rebound? Or is it necessary that the bodies possess some "springiness"? Wallis and Mariotte concluded that springs are necessary, while Huygens, Wren, and Malebranche thought that hardness is sufficient [1307]. We know now the difference between a model of nature and nature itself. We also have many more mathematical

[1] However, in many practical cases it is very short: 4.10^{-4} s for a shock between a golf ball and a flat-nosed wooden projectile with a relative speed of 5.334 m/s [196], other authors report values between 7.10^{-4} and 5.10^{-4} s for pre-impact velocities between 10 and 60 m/s [55]; see other values of the same order in Sect. 4.3.10 for slender rods against a massive steel table.

B. Brogliato, *Nonsmooth Mechanics*, Communications and Control Engineering,
DOI 10.1007/978-3-319-28664-8_2

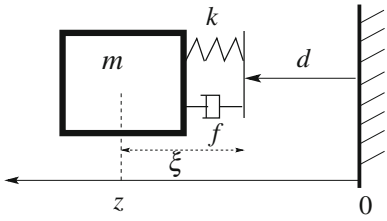

Fig. 2.1 Linear spring/dashpot contact-impact model

tools at our disposal to accept perfect rigidity and to study accurately the relationship between compliant and rigid models.[2]

2.1 Simple Examples

This section is dedicated to the analysis of the simplest compliant contact model: parallel linear spring-dashpot assemblies. Several of their properties are studied: convergence when parameters tend to infinity (rigid body limit), equivalent restitution coefficient, complementarity formalism, well-posedness of simple dynamics incoportating such piecewise-linear models. The considered models possess a mathematical interest where they may be used for existence/uniqueness of solutions proofs, as illustrated in the second part of this chapter. It is noteworthy that the following analysis also holds for two particles moving on a line and colliding, adapting the masses, stiffnesses and damping coefficients to their equivalent (or effective) values. For instance, the effective mass is $m = \frac{m_1 m_2}{m_1+m_2}$, the equivalent stiffness is $k = \frac{k_1 k_2}{k_1+k_2}$, the equivalent damping coefficient is $f = \frac{f_1 f_2}{f_1+f_2}$, for two spring-dashpot systems as on Fig. 2.1 mounted in series.

2.1.1 From Elastic to Hard Impact

Consider that we attach a linear spring with stiffness k to the mass m moving on a horizontal line, and that the mass collides with a wall (infinite mass) through the spring, at time t_0 (take $f = 0$ in Fig. 2.1). The position of the mass is z, and $\xi = l$ corresponds to the spring at rest. Let $k > 0$ be its stiffness, m is the mass. If the spring was a bilateral spring capable of exerting positive and negative forces F on the mass, one would have $F = k(l - \xi)$, so that $F > 0$ if $l - \xi > 0$ (compressed spring, repulsive contact force), and $F < 0$ if $l - \xi < 0$ (stretched spring, attractive contact force). However, in our case the spring is unilateral, which means that it may detach from the "wall". During the contact phases of motion, the spring is compressed, i.e., $l - \xi > 0$, while $z = \xi$, so that $F = k(l - \xi) = k(l - z) > 0$. During non

[2] Although, as we shall see, this still requires advanced mathematical studies.

contact phases one has $F = 0$ and $z > \xi$, while $\xi = l$ since the spring is massless (it has no dynamics by itself). Doing the change of variable $x = z - l$ one obtains $F(x) = 0$ if $x \geq 0$, and $F(x) = -kx$ if $x \leq 0$. The dynamics of the mass is given by $m\ddot{x}(t) = F(x(t))$. Therefore one obtains:

$$\begin{cases} m\ddot{x}(t) = 0 & \text{if } x(t) \geq 0 \\ \\ m\ddot{x}(t) + kx(t) = 0 & \text{if } x(t) \leq 0. \end{cases} \tag{2.1}$$

This model yields a multivalued stiffness, as explained in Example 1.6, Remark 1.7. Assume that the spring remains in contact with the wall on the time interval $[t_0, t_1]$, i.e. t_0 is the instant when the mass/spring system makes contact with the wall, and t_1 the time when it detaches. One has $x(t_1) = x(t_0) = 0$, and $\dot{x}(t_0) = \dot{x}_0 < 0$ while $\dot{x}(t_0) > 0$. Let us set $t_0 = 0$. We obtain during the contact phase $[0, t_1]$: $x(t) = \dot{x}_0\sqrt{\frac{m}{k}}sin(\sqrt{\frac{k}{m}}t)$. The first time instant after the impact such that $x(t_1) = 0$ is the impact duration:

$$t_1 = \sqrt{\frac{m}{k}}\pi. \tag{2.2}$$

(i.e. the spring is being crushed and then restores its potential energy). Note that $\dot{x}(t_1) = -\dot{x}_0 > 0$. Consider now any sequence of stiffness values $\{k_n\}$, $n \in \mathbb{N}$, $k_n < k_{n+1}$, $k_n \to +\infty$ as $n \to +\infty$. Let us denote $F_n(\tau) = -k_n x_n(\tau)$ for $0 \leq \tau \leq t_1$, $F_n(\tau) \equiv 0$ elsewhere. Note that the subscript n in $x_n(t)$ is to emphasize that $x_n(t)$ is the solution of an approximating problem with stiffness k_n. Then, $\int_0^{t_1} F_n(\tau)d\tau = -\int_0^{t_1} k_n x_n(\tau)d\tau = 2|\dot{x}_0|m > 0$ for all $n > 0$. Now notice that $x_n(\tau) \to 0$ on $[0, t_1]$ as $n \to +\infty$ and $t_1 \to 0^+$ as $n \to +\infty$, i.e., if the stiffness is infinite, $x(\cdot)$ remains unchanged during the impact[3] and the impact duration is zero. Moreover, the compliant elastic collision tends towards a hard (i.e., purely elastic and instantaneous) collision. It is easy to verify that the sequence $F_n(\cdot)$ of contact force functions converges to $2|\dot{x}_0|m\delta_0$ as $n \to +\infty$, by checking conditions **i**, **ii** and **iii** for delta-sequences given in Appendix A.1, Sect. A.1.2.

Following the terminology used in most mathematical studies [241, 242, 260, 989, 990] we have chosen a *penalizing function* $F_n(x_n) = -k_n x_n$ if $x_n > 0$, 0 if $x_n \leq 0$, that exactly fits within the conditions imposed by these authors.

2.1.1.1 The Work Performed by Contact Forces

The work effectuated by the contact force during the impact is given by $W_{[0,t_1]} = \int_0^{t_1} \dot{x}_n(t)k_n x_n(t)dt = \frac{m\dot{x}_0^2}{2}[cos^2(\pi) - 1] = 0$ for any $k_n \in \mathbb{R}^+$. Thus, it seems reasonable to consider that the work of the impulsive force at the impact time is zero.

[3] Constant positions is a common assumption in impact mechanics.

This is consistent with the lossless property of this model. The maximum interaction force value is given by:

$$F_{\max} = |\dot{x}_0|\sqrt{km}, \tag{2.3}$$

and therefore tends to infinity as the stiffness k grows unbounded. Thus, the intuitive and widely spread idea of "very large" forces at impacts seems quite justified from this mathematical model. The correct idea is to consider the effect of the interaction force $F(\cdot)$ as a distribution in $\mathscr{D}^\star$. One sees that the action on any function in $\mathscr{D}$ with support containing 0 is finite, for any k, because the support of $F(\cdot)$ tends towards zero so that $F(\cdot)$ becomes atomic. As we have already seen, what is to be considered as the impact magnitude for infinitely large k is the magnitude p of the impulse, which exactly corresponds to the integral of the interaction force over the contact interval (i.e., what is called the impulse of the interaction force during the contact period), and not to the maximum value of this force, that makes no sense when $k = +\infty$. However, for practical purposes one may also argue that the maximum value of the interaction force is important (to be able to prevent possible damage of the materials in contact). Then it is clear that a rigid body model cannot predict such value, and one has to use a suitable compliant approximating model of the contact-impact process.

Remark 2.1 When a constant force F_0 acts on the mass, it is still possible [591] to calculate the solution as $x(t) = \frac{F_0}{k}(1 - \cos(\sqrt{k}t)) + \frac{\dot{x}_0}{\sqrt{k}}\sin(\sqrt{k}t)$, the impact duration as $t_1 = \frac{2}{\sqrt{k}}\arctan\left(-\frac{\sqrt{k}}{F_0}\dot{x}_0\right)$, and the impulsion of the contact force as $P(t_1) = -2\dot{x}_0 + 2\frac{F_0}{\sqrt{k}}\arctan\left(\frac{\sqrt{k}}{F_0}\dot{x}_0\right)$.

2.1.1.2 Complementarity Modelling

Unilaterality is present in the model since the contact force is set to zero when $x > 0$. One says that the contact model is a unilateral linear spring. Let the dynamics be expressed as: $m\ddot{x}(t) - \lambda(x(t)) = 0$, where $\lambda(x)$ is defined as follows:

$$\lambda(x) = \begin{cases} 0 & \text{if } x \geq 0 \\ -kx & \text{if } x \leq 0 \end{cases} \quad \Leftrightarrow \quad \lambda(x) = \max(0, -kx)$$

$$\Leftrightarrow \quad 0 \leq \lambda(x) \perp w(x) = \lambda(x) + kx \geq 0 \quad \Leftrightarrow \quad \lambda(x) = \operatorname{argmin}_{z \geq 0} \tfrac{1}{2}(z + kx)^2, \tag{2.4}$$

where $\perp$ means that the two variables $\lambda(x)$ and $w(x)$ have to be mutually orthogonal: in the scalar case this is simply $\lambda(x)w(x) = 0$. The third formalism in (2.4) is called a *Linear Complementarity Problem* (LCP), a formalism we already met in Example 1.6. The equivalences may be checked by inspection: if $x > 0$, then $-kx < 0$ and the only solution is $\lambda(x) = kx > 0$. If $x < 0$ then $-kx > 0$ and the only solution is $\lambda(x) = 0$. The case $x = 0$ yields $\lambda(0) = 0$. The equivalence with the quadratic program is a consequence of the Karush-Kuhn-Tucker (KKT) conditions which yield

the equivalence between (5.107) and (5.109) in Sect. 5.4.3. The equivalences in (B.19) and (B.20) in the Appendix may also be used. The dynamics of the mass may therefore be written as

$$\begin{cases} m\ddot{x}(t) + \lambda(t) = 0 \\ 0 \leq \lambda(t) \perp w(\lambda(t), x(t)) = \lambda(t) + kx(t) \geq 0, \end{cases} \tag{2.5}$$

which is a simple example of a *Linear Complementarity System*. Obviously the multiplier λ in (2.5) is a function of x, being the solution of the above LCP. It is even a Lipschitz continuous function of x, according to Theorem 5.4. To complete this section, let us notice that the complementarity conditions may be written equivalently as $0 \leq w(t) \perp \lambda(t, x(t)) = w(t) - kx(t) \geq 0$, with $m\ddot{x}(t) = w(t) - kx(t)$ and $\lambda(t) = w(t) - kx(t)$. The distance between the mass + spring-dashpot and the wall is $d(t) \geq 0$, with $d(t) = x(t)$ if $x(t) \geq 0$, and $d(t) = 0$ if $x(t) < 0$. So, we have in fact $w(t) = kd(t)$, so that $0 \leq d(t) \perp d(t) - x(t) \geq 0$. In view of this, since $\lambda(t) = \frac{1}{k}(d(t) - x(t))$, we have that $0 \leq d(t) \perp \lambda(t) \geq 0$, which states the complementarity between the contact force and the distance between the mass and the obstacle: this is a formalism which we will meet all through the book, especially for rigid bodies.

2.1.2 From Damped to Plastic Impact

Let us now assume that only a damper is attached to the mass, with viscous friction coefficient $f > 0$, as shown in Fig. 2.1. The contact force exerted by the viscous friction is $F(\dot{z}) = -f\dot{\xi}$ if $z = \xi$, $F = 0$ if $z > \xi$. Doing the same variable change $x = z - l$ as in Sect. 2.1.1, one obtains

$$\begin{cases} 0 \leq t \leq t_c : m\ddot{x}(t) = 0 \\ \\ t_c \leq t \leq t_1 : m\ddot{x}(t) + f\dot{x}(t) = 0, \end{cases} \tag{2.6}$$

where t_c is the instant when the mass/dashpot system makes contact with the wall. Proceeding as above, we obtain after the impact time $\dot{x}(t) = \dot{x}_0 e^{-\frac{f}{m}t}$, $x(t) = -\frac{m\dot{x}_0}{f}(1 - e^{-\frac{f}{m}t})$. One sees that if $f \to +\infty$, then $x(t) \to x(0) = 0$ and $\dot{x} \to 0$ for all $t > 0$. For any sequence of values of damping coefficient $\{f_n\}$ defined as in the preceding example, let us denote $F_n(\tau) = f_n\dot{x}_n(\tau) + m\dot{x}_0\sqrt{\frac{f_n}{m}}\mathrm{e}^{-\sqrt{\frac{f_n}{m}}}$ for $0 \leq \tau \leq \sqrt{\frac{m}{f_n}}$, $F_n(\tau) \equiv 0$ elsewhere. Then, $\int_0^{\sqrt{\frac{m}{f_n}}} F_n(\tau)d\tau = \int_0^{+\infty} f_n\dot{x}_n(\tau)d\tau$. Note that this time the interaction impulse is calculated on the whole interval $[0, +\infty)$ since the body never detaches from the surface after contact has been established. It is easy to check that $F_n(\cdot)$ satisfies conditions **i**, **ii** and **iii** in Appendix A.1. Hence, we get $F_n(\cdot) \to m\dot{x}_0\delta_0$ as $n \to +\infty$. In the limit, the equation describing the system with one impact at $t = 0$ becomes the MDE $m\ddot{x} = \{\ddot{x}(t)\}dt + m\sigma_{\dot{x}}(0)\delta_0$, with

$\{\ddot{x}(t)\} = 0$ (null acceleration outside the impact time), $\sigma_{\dot{x}}(0) = -\dot{x}(0^-) = -\dot{x}_0$ since $\dot{x}(0^+) = 0$.

2.1.3 The General Case

2.1.3.1 The "Usual" Switching Conditions

Consider now that we attach a spring $k > 0$ and a damper $f > 0$ to the mass as in Fig. 2.1.[4] Proceeding exactly as in the previous two cases, the dynamics during the contact phases of motion is given by

$$\begin{cases} m\ddot{x}(t) + f\dot{x}(t) + kx(t) = 0 \ \text{ if } \ x(t) \leq 0 \\ \\ m\ddot{x}(t) = 0 \ \text{ if } \ x(t) > 0, \end{cases} \tag{2.7}$$

hence, a discontinuous vector field if $\dot{x}(t) \neq 0$ at the transition time. Let us assume that $\Delta \stackrel{\Delta}{=} f^2 - 4km < 0$. Thus, we obtain with the same initial conditions as in the undamped case $x(t) = \frac{\dot{x}_0}{\omega} e^{rt} sin(\omega t)$, $\dot{x}(t) = \dot{x}_0 e^{rt} \left[\frac{r}{\omega} sin(\omega t) + cos(\omega t)\right]$, with $\dot{x}_0 = \dot{x}(0) < 0$, $r = \frac{-f}{2m}$, $\omega = \frac{\sqrt{-\Delta}}{2m}$. The time instant

$$t_1 = \frac{\pi}{\omega} = \pi \left(\frac{k}{m} - \left(\frac{f}{2m} \right)^2 \right)^{-\frac{1}{2}} \tag{2.8}$$

at which $x(t_1) = 0$ and $\dot{x}(t_1) = -\dot{x}_0 e^{\frac{r\pi}{\omega}}$, furnishes the impact duration. Let us choose $0 < \beta \leq 1$, and let us see what happens if[5]:

$$f = 2|ln(\beta)| \left(\frac{km}{\pi^2 + ln^2(\beta)} \right)^{\frac{1}{2}}, \tag{2.9}$$

when $k \to +\infty$ (Such an f guarantees $\Delta < 0$ for $0 < \beta \leq 1$): we get $t_1 \to 0$ and $e^{\frac{r\pi}{\omega}} \to \beta$. Thus, $\dot{x}(t_1) \to -\beta \dot{x}_0$ as $k \to +\infty$ (if $\beta = 1$ then $f \equiv 0$ and we retrieve the above case, and if $0 < \beta < 1$, then $f \to \infty$ as $k \to \infty$). Simple calculations show that $\int_0^{\frac{\pi}{\omega}} F_n(\tau) d\tau \stackrel{\Delta}{=} -\int_0^{\frac{\pi}{\omega}} (f_n \dot{x}_n(\tau) + k_n x_n(\tau))\, d\tau = m|\dot{x}_0|(\beta + 1)$, where $\{k_n\}$ is a sequence of stiffness coefficients defined as previously, and $f_n = 2|ln(\beta)| \left(\frac{k_n m}{\pi^2 + ln^2(\beta)} \right)^{\frac{1}{2}}$. Thus, once again the sequence of force functions $F_n(\cdot)$ during the collision time converges towards a Dirac distribution. Note that to show this, we have considered a sequence of damping coefficients that depend on the mass m. This

[4] This model is often called a *linear spring-dashpot* model, or the Kelvin-Voigt model.

[5] Let us note that the following relationship means that the damping coefficient is taken to be proportional to the square root of the stiffness coefficient.

is at first sight surprizing, as one can expect the nature of collision to be dependent not only on the mass of the bodies that collide, but also on the approach velocity. However, what really matters in this analysis is not how the sequences $\{f_n\}$ and $\{k_n\}$ are defined but rather that they do exist, i.e., we are able to associate a sequence of compliant models to the rigid limiting model.

Remark 2.2 (*Impact duration*) The above calculations show that the impact characteristic time is $\mathcal{O}(\frac{1}{\sqrt{k}})$. As shown in [969] this remains true for a Lagrangian system with a single contact and a linear spring-dashpot model. This is only a crude approximation of experimental data, where it is known that the impact time depends on the pre-impact velocity, see Remark 4.6.

Note that when $\beta \to 0$, $\beta > 0$, then $\Delta \to 0$, $\Delta < 0$, $f \to 2\sqrt{km}$, and as $k \to +\infty$ (the sequence $\{k_n\}$ can be chosen of the form $k_n = k_n^{'} \ln^2(\beta)$, with $k_n^{'} \to +\infty$) then $t_1 \to 0$ and $\dot{x}(t_1) \to 0$ also. More formally, let us define a sequence of positive coefficients β_j, with $\beta_j \to 0$ as $j \to +\infty$. Hence we define the functions $p_{n,j}(t) = -f_{n,j}\dot{x}_{n,j}(t) - k_{n,j}x_{n,j}(t)$. Then, from the above it follows that $F_{n,j}(\cdot) \to m\dot{x}_0(\beta_j + 1)\delta_0 = p_j\delta_0$ and trivially $p_j\delta_0 \to m|\dot{x}_0|\delta_0$ as $j \to +\infty$ (convergence is always understood in the sense of distributions, see Appendix A.1, Sect. A.1.3). Therefore, $F_{n,j}(\cdot) \to m\dot{x}_0\delta_0$ as n and $j \to +\infty$. We have thus found two different sequences of interaction forces, both based on simple mechanical models of contact-impact that both approximate the same limit problem, i.e., a purely inelastic shock.

Remark 2.3 (*Contact Force with Wrong Sign*) The contact force is $F(x, \dot{x}) = -kx - f\dot{x}$ for $x \leq 0$. Normally, we should have $F(x(t), \dot{x}(t)) \geq 0$ during an impact, because no adhesive effects have been modeled with such a linear spring-dashpot assembly. During the compression phase one has $\dot{x}(t) < 0$ so that $-f\dot{x}(t) > 0$ and $F(x(t), \dot{x}(t)) > 0$: the acceleration $\ddot{x}(t)$ is positive, since $\dot{x}(0) < 0$ the velocity increases until it vanishes (maximum compression time) and reverses its sign so that the expansion phase starts. However, during the expansion phase $\dot{x}(t) > 0$ so that the dissipative force $-f\dot{x}(t) < 0$. Close to the detachment position, $x(t)$ is very small and there always exists a position, hence a time, before the detachment occurs, at which the dissipative force dominates the elastic one. Therefore, it is always the case that before detachment, $F(x(t), \dot{x}(t)) < 0$ and this persists until the detachment time occurs, see Fig. 2.4b. Notice anyway that if the contact model guarantees that the impact finishes at some time t_1 with $\dot{x}(t_1) \geq 0$, with an initial velocity $\dot{x}(0) < 0$, then $m(\dot{x}(t_1) - \dot{x}(0)) = \int_{[0,t_1]} F_{\mathrm{n}}(t)dt = p_{\mathrm{n}}(t_1) > 0$, despite possibly negative contact force. This holds for any model satisfying such "collision" assumption.

We have calculated the final collision time as being the first time t_1 when $x(t_1) = 0$. One drawback of this choice is that the force exerted by the spring-dashpot on the mass, may become negative during the impact. This is a nonphysical behavior. This has motivated the choice of another criterion for the end of the impact [239, 274, 474, 475, 1079, 1080], as the first time $t = t_f \neq t_1$ when the contact force vanishes, i.e.,[6]: $f\dot{x}(t_f) + kx(t_f) = 0$. This yields an expression for the ratio $\beta = -\frac{\dot{x}(t_f)}{\dot{x}(t_0)}$ of the

[6] We will see in Sect. 2.1.3.4 that this approach is to be embedded into a complementarity model.

rebound velocity versus the initial one, called the *restitution coefficient*,[7] different from that in (2.9). One finds:

$$\beta = \exp\left(-\frac{\zeta}{\sqrt{1-\zeta^2}}\arccos\left(2\zeta^2-1\right)\right) \tag{2.10}$$

where $\zeta = \frac{f}{2m\omega}$, $\omega = \sqrt{\frac{k}{m}}$, and $0 \leq \zeta < 1$. Further expressions may be calculated for less damped systems with $\zeta \geq 1$ [274]. One obtains for $\zeta > 1$:

$$\beta = \frac{1}{4\zeta\sqrt{\zeta^2-1}}\eta^{-\frac{\zeta}{\sqrt{\zeta^2-1}}}\left(\eta - \frac{1}{\eta}\right), \quad \eta = \sqrt{\frac{2\zeta^2-1+2\zeta\sqrt{\zeta^2-1}}{2\zeta^2-1-2\zeta\sqrt{\zeta^2-1}}}, \tag{2.11}$$

instead of (2.10). Let us come back to the switching conditions in (2.7). Inverting (2.9) the restitution coefficient may be found as:

$$\beta = \exp\left(-\frac{\pi\zeta}{\sqrt{1-\zeta^2}}\right) = \exp\left(-\frac{\pi\mu}{\sqrt{\omega_0^2-\mu^2}}\right), \tag{2.12}$$

where $\zeta = \frac{f}{2\sqrt{km}}$ is supposed to be in $[0, 1]$, $\omega_0 = \sqrt{\frac{k}{m}}$, $\mu = \frac{f}{2m}$ (if the dynamics is equivalently written as $\ddot{x}(t) + 2\mu\dot{x}(t) + \omega_0^2 x(t) = 0$). If $\zeta > 1$ then the restitution coefficient $\beta = 0$ [1080]. It is obvious that β in (2.12) varies from 1 ($\zeta = 0$) to 0 ($\zeta = 1$). It is remarkable that changing the switching surface, changes significantly the equivalent restitution property. As will be seen next, the mathematical analysis differs as well.

Let two one-degree-of-freedom particles collide each other, and one associates a spring-dashpot contact model with each of them. The basic model we used above may be recovered by setting equivalent stiffness $k = \frac{k_1 k_2}{k_1+k_2}$, equivalent damping $f = \frac{f_1 f_2}{f_1+f_2}$, and equivalent mass $m = \frac{m_1 m_2}{m_1+m_2}$, with the coordinate $x = x_1 - x_2$. Newton's third law on action/reaction is used as well.

2.1.3.2 The Work Performed by Contact Forces

The work performed by the contact forces during the impact is given this time by $W_{[0,t_1]} = \int_0^{t_1} \dot{x}_n(t)(f_n\dot{x}_n(t) + k_n x(t))dt = \frac{1}{2}\frac{k\dot{x}_0^2}{\omega^2+r^2}\left[e^{\frac{2r\pi}{\omega}} - 1\right]$ that tends towards $\frac{m\dot{x}(0)^2}{2}(\beta^2 - 1) < 0$ when $k \to +\infty$. We will see later in the book that this quantity is exactly the loss of kinetic energy T_L at impact and can also be deduced from

[7] This restitution coefficient will be denoted as e_n in the rest of the book, where the subscript n is for "normal".

the result in [1192] that states that the work performed by the impact of a particle against a massive barrier is given by an "average" formula $W_{[0,t_1]} = P_{\mathrm{n}}(t_1)\frac{\dot{x}(t_1)+\dot{x}(0)}{2}$ where $P_{\mathrm{n}}(\cdot)$ is the normal impulse of the percussion, i.e., the time integral of the interaction force during the shock interval (thus $P_{\mathrm{n}}(0) = 0$). See Chap. 4 for further developments on the Thomson and Tait formula.

Thus, once again the approximating model allows us to give a meaning to the impulsive work that is consistent with the energetical behavior of the impact (here a loss of energy as long as $\beta < 1$). Note that the distributional formulation permits to calculate easily the loss of kinetic energy but not the impulsive forces work. This is somewhat paradoxical since both quantities are equal and represent the same physical process of energy dissipation. Actually, one needs a generalization of the vis-viva Theorem which states (for smooth motions) that $W_{[t_0,t_1]} = \int_{t_0}^{t_1} F(t)^T \dot{x}(t)dt = T(t_1) - T(t_0)$. The work performed by impulsive forces is sometimes deduced from (1.1) as $W_k = \lim_{\Delta t\to 0}\int_{t_c}^{t_c+\Delta t} p_{\mathrm{n}}(\tau).\dot{x}(\tau)d\tau$: it is clear that without any approximating sequence of impact problems, the integrand is meaningless in the distributional sense. Let us denote the restitution coefficient β as e_{n}. We have proved the following:

Proposition 2.1 *Consider the equation in (1.2) that represents the dynamics of a rigid mass colliding a rigid environment, without any external action. Then, for any energetical behavior of the materials at the impacts (namely for any restitution coefficient* $0 \leq e_{\mathrm{n}} \leq 1$*) we can associate an approximating sequence of compliant models such that the approximating solutions* $x_n(\cdot)$ *converge uniformly towards the solution of (1.2).*

Roughly speaking, as we pointed out in Remark 1.1, we have approximated the limit rigid problem by sequences of differential equations of the form $m\ddot{x}_n(t) = F_n(t)$ for a given sequence of functions $\{F_n(t)\}$, whose limit is a Dirac measure. Results for convergence of this kind may be found for instance in [397, Chap. 1] (see in particular Lemmas 4 and 5 §1, Theorem 1, §2 in that book). Uniform convergence can be proved by using the change of variables indicated in Examples 1.1 and 1.3 since the resulting system is Carathéodory. This holds for $x_n(\cdot)$ only since $\dot{x}_n(\cdot)$ is continuous and cannot thus converge uniformly to a discontinuous $\dot{x}(\cdot)$. The result holds for more general systems like the one in Example 1.3 as long as the "impact function" $h(t)$ is of local bounded variation.[8] We have been able to prove the above because the considered problem is integrable and the exit times can be calculated. As pointed out in the previous section, in the general case the problem is much more involved. A possible work is to find out arguments proving that sequences $\{f_n\}$ and $\{k_n\}$ exist that yield the same results when for instance an external force $u(t)$ acts on the system. As an illustration, consider the classical bouncing ball problem, that corresponds to adding a constant force (gravity) to the mass: then it can be shown that the impulsive force acting on the ball for $0 < e_{\mathrm{n}} < 1$ has the form $F = \sum_{k=0}^{+\infty} p_k\delta_{t_k}$, where $t_\infty < +\infty$ is

[8] Strictly speaking, this fact has to be proved. In the simple examples we have treated, we have been able to integrate the equations and to calculate the functions $F_n(\cdot)$. Obviously, in slightly more complex cases this would not be possible.

an accumulation point of the sequence $\{t_k\}$. A fundamental property of this sequence is that the step function $h(t) \stackrel{\Delta}{=} \sum_{k=0}^{n} p_k$ on $[t_n, t_{n+1}]$, $n \geq 0$ is of bounded variation on $[t_0, t_\infty]$. Hence, from [1082, p. 25, Theorem 2, p. 53] $p = \dot{h}$ can be considered as a Schwartz's distribution since it is a bounded measure. Then, from density of $\mathscr{D}$ in $\mathscr{D}^\star$ [1082, Theorem 15, Chap. 3], we can approximate p and h by sequences of smooth functions $\{p_n\}$ and $\{h_n\}$. From [51, Lemma 2.2.5], $\dot{h}_n = p_n$ since the functions $\dot{h}_n$ are continuous. Are there sequences of damping and stiffness coefficients such that the corresponding compliant model is an approximating sequence for this problem? The work in [969] that we describe later yields a positive answer.

2.1.3.3 Well-Posedness of (2.7)

The system in (2.7) is a switching dynamical system, whose vector field is discontinuous on the switching surface $\Sigma = \{(x, \dot{x}) | x = 0\}$. It is easy to add an external action $F(t)$ to the dynamics (2.7). Let $z_1 = x$ and $z_2 = \dot{x}$, then one may rewrite (2.7) as a first-order switching system $\dot{z}(t) = A_1 z(t) + BF(t)$ if $z_1(t) \leq 0$, $\dot{z}(t) = A_2 z(t) + BF(t)$ if $z_1(t) \geq 0$. On the switching surface Σ, the vector field jumps with a discontinuity equal to $(A_1 - A_2)z(t)$ and $z_1(t) = 0$, so that $(A_1 - A_2)z(t) = (0 \ \frac{-f}{m} z_2(t))^T$. It is possible to embed this system into the general framework of Filippov's differential inclusions, just as the systems of Sect. 1.4.3. Then, one rewrites it as:

$$\dot{z}(t) \begin{cases} = A_1 z(t) + BF(t) \ \text{ if } \ z_1(t) \leq 0 \\ = A_2 z(t) + BF(t) \ \text{ if } \ z_1(t) \geq 0 \\ \\ \in \overline{\text{conv}}(A_1 z(t), A_2 z(t)) \ \text{ if } \ z_1(t) = 0, \end{cases} \tag{2.13}$$

where $\overline{\text{conv}}(A_1 z(t), A_2 z(t))$ is the closure of the convex hull of the two vectors. It is found to be $\text{conv}(A_1 z(t), A_2 z(t)) = \{v \in \mathbb{R}^2 | v = \begin{pmatrix} z_2(t) \\ \frac{-\alpha f}{m} z_2(t) + F(t) \end{pmatrix}, \alpha \in [0, 1]\}$. It is noteworthy that the Filippov's convexification, or regularization method, disregards the value of the vector field on the switching surface Σ. It is therefore not important whether the inequalities defining the switching conditions, are strict or not in (2.7). Due to the way Filippov's right-hand side is constructed, the following holds:

Lemma 2.1 *The differential inclusion in (2.13) possesses for each initial condition* $(z_1(0), z_2(0))$ *an absolutely continuous solution which satisfies the inclusion for almost all* $t \geq 0$.

The simplest example of a Filippov's convexification is the discontinuous system $\dot{z}(t) = 1$ if $z(t) > 0$, $\dot{z}(t) = -1$ if $z(t) < 0$. Then one obtains the differential inclusion $\dot{z}(t) \in \text{sgn}(z(t))$ where $\text{sgn}(\cdot)$ is the set-valued signum function, equal to $\partial|\cdot|$ (see Sect. B.1). There exist other ways to characterize the solutions of (2.7), for instance considering that on Σ one has $\dot{z}(t) \in \{A_1 z(t), A_2 z(t)\}$, i.e., two

values are assigned to the vector field instead of a whole segment. This gives rise to Carathéodory solutions [1197].

What about uniqueness property? The so-called *one-sided Lipschitz* condition for set-valued mappings [13] secures uniqueness of solutions for differential inclusions. However, one may check using [1197, Theorem 2.6] that the mapping in the right-hand side of (2.13) is not one-sided Lipschitz continuous. The criteria in [1197, Theorems 3.1, 3.3, 3.4, Corollary 3.5] may be used to test the uniqueness property. If $F(t) = 0$ [1197 Corollary 3.5] applies and uniqueness of solutions of (2.13) in the sense of Filippov holds. Carathéodory solutions are analyzed in [574].

The Zeno behavior may be characterized through [1197, Theorem 4.2]. Let us remind that the system (2.13) is non-Zeno if the switches, i.e., the time instants when Σ is crossed, are well-separated one from each other. In particular they never accumulate. The criterion in [1197, Theorem 4.2] consists of constructing three equations from "observability" matrices $(C^T\ C^T A_1\ C^T A_1^2)^T$ and $(C^T\ C^T A_2\ C^T A_2^2)^T$, where the switching function $C^T z = (1\ 0)z$ is seen as an output. When applied to (2.13) it yields non-Zenoness provided $F(t) = 0$.

Remark 2.4 The criteria in [1197] rely strongly on observing the derivatives of the switching function, on the switching surface, and characterizing them through lexicographical inequalities. This is an ubiquitous tool for the analysis of switching and unilaterally constrained systems.

2.1.3.4 Complementarity Modelling

The model in Sect. 2.1.1.2 assumes that the switches occur when $x(\cdot)$ crosses the zero value, see (2.7). Let us consider now the other switching condition for the linear spring-dashpot model that yields the restitution coefficient in (2.10). It allows one to eliminate the phases of motion where the contact force may become negative, a phenomenon that is observed with the "usual" swicthing conditions as noted in Remark 2.3 (see also Fig. 2.4b). During the contact phases one still has $z(t) = \xi(t)$ and $F(z, \dot{z}) = -f\dot{z} - k(z - l) = -f\dot{x} - kx$ with $x \stackrel{\Delta}{=} z - l$, and $x(t) \leq 0$. Let us set the following dynamics:

$$\begin{cases} \dot{\eta}(t) = A\eta(t) + B\lambda(t) \\ \\ 0 \leq w(\eta(t)) = C\eta(t) \perp \lambda(t) \geq 0, \end{cases} \tag{2.14}$$

where $\eta^T = (x, \dot{x}, \bar{\xi})$, $\bar{\xi} = \xi - l$, $A = \begin{pmatrix} 0 & 1 & 0 \\ 0 & 0 & 0 \\ 0 & 0 & -\frac{k}{f} \end{pmatrix}$, $B^T = \begin{pmatrix} 0 & \frac{1}{m} & -\frac{1}{f} \end{pmatrix}$, $C = \begin{pmatrix} 1 & 0 & -1 \end{pmatrix}$. The matrix A has two zero eigenvalues and one eigenvalue equal to $-\frac{k}{f}$, and is thus marginally stable. The variable $w(\eta) = z - \xi = x + l - \xi = x - \bar{\xi}$ represents the signed distance between the spring-dashpot system and the constraint,

while ξ is the deformation of the spring and the damper. The contact and noncontact phases correspond to $w(\eta) = 0$ ($\Rightarrow \lambda(\eta) \geq 0$) and $w(\eta) > 0$ ($\Rightarrow \lambda(\eta) = 0$) respectively. During noncontact phases, the spring-dashpot system has the dynamics $\dot{\bar{\xi}}(t) = -\frac{k}{f}\bar{\xi}(t)$, equivalently $f\dot{\xi}(t) = -k(\xi(t) - l)$. Contarily to the undamped case, where $f = 0$ implies $\xi = l$, it has its own dynamics, though it is massless.

The obtained system in (2.14) is a Linear Complementarity System. There is a significant difference between (2.14) and (2.5): in (2.14) the multiplier $\lambda(\eta)$ does not appear in both sides of the complementarity conditions, hence one cannot use straightforwardly the equivalences in (2.4) to compute its value. One has to differentiate once the variable $w(\eta)$ to recover a Linear Complementarity Problem (LCP, see Definition 5.105). If $w(\eta(t)) = C\eta(t) = 0$ on $[t', t'']$, for some $t'' > t'$, then the complementarity condition $0 \leq \dot{w}(t) = C\dot{\eta}(t) \perp \lambda(\eta(t)) \geq 0$ holds on (t', t'').[9] Since $CB = \frac{1}{f} > 0$, $\lambda(\eta(t))$ is at time $t \in [t', t'']$ the unique solution of the LCP:

$$0 \leq \lambda(\eta(t)) \perp \dot{w}(t) = CA\eta(t) + CB\lambda(\eta(t)) \geq 0, \tag{2.15}$$

whose matrix $CB = \frac{1}{f}$ is obviously a P-matrix (see Theorems 5.4 and 5.5). Let $CA\eta(t) = \dot{x}(t) + \frac{k}{f}\bar{\xi}(t) \leq 0$, then the multiplier is given by $\lambda(\eta) = -fCA\eta(t) = -f\dot{x}(t) - kx(t) \geq 0$, noting that during this phase of the motion one has $z(t) = x(t)+l = \xi(t)$. If we have on the contrary $CA\eta(t) \geq 0$ then the multiplier is $\lambda(t) = 0$: there is a detachment from the obstacle at the time instant t_f when $CA\eta(t_f) = 0$, i.e., the force exerted by the obstacle (the spring-dashpot system) on the mass vanishes and then takes negative values.

One may say that the *relative degree* between the "output" $w(\eta)$ and the "input" $\lambda(\eta)$ is equal to zero in (2.5) and equal to one in (2.14).

$\rightsquigarrow$ *It is noteworthy that in both* (2.14) *and* (2.5), *transitions from noncontact to contact occur with a continuous state and a bounded multiplier (contact force)* λ. *There is no state jumps nor Dirac measure.*

To summarize, noncontact phases of motion have the dynamics $\dot{\eta}(t) = A\eta(t)$, while contact phases have the dynamics $\dot{\eta}(t) = \begin{pmatrix} 0 & 1 & 0 \\ \frac{-k}{m} & \frac{-f}{m} & 0 \\ \frac{k}{m} & 1 & \frac{-k}{m} \end{pmatrix} \eta(t)$. Since in the contact phase one has $w(t) = 0 \Leftrightarrow z(t) = \xi(t) = x(t) + l$, the ξ-dynamics reduces to $\dot{\xi}(t) = \dot{z}(t) = \dot{x}(t)$ which trivially holds. The rest of the dynamics is that of a mass with stiffness and damping effects.

Well-Posedness Analysis

Let us refer to Theorem 5.4 in Sect. 5.4.2, which stipulates that $\lambda(x)$ as a solution of the LCP in (2.5), is a Lipschitz continuous function of x. It follows that the system in (2.5) is an Ordinary Differential Equation with Lispchitz continuous vector field (this

[9] Here $\dot{w}(t) = \nabla w(\eta)^T \dot{\eta}(t)$.

continues to hold if an external action $F(t)$ is added, provided $F(t)$ is regular enough). Hence general results about existence, uniqueness and continuous dependence apply to the Linear Complementarity System (2.5), which possesses continuously differentiable solutions. The system (2.5) may also be seen as a piecewise-linear system with continuous vector field. Such straightforward conclusion cannot be drawn for (2.14), which requires more analysis, as in particular its vector field is no longer continuous at the switching surface. Let us first notice that using (B.19) one obtains that (2.14) is equivalent to the differential inclusion:

$$\dot{\eta}(t) - A\eta(t) \in -B\ N_{\mathbb{R}_+}(C\eta(t)). \tag{2.16}$$

A useful relation is that there exists a symmetric, positive definite matrix P such that $PB = C^T$.[10] For instance the matrix:

$$P = \begin{pmatrix} p_{11} & m & 0 \\ m & 1 & \frac{f}{m} \\ 0 & \frac{f}{m} & \frac{f^2}{m^2} + f \end{pmatrix}, \quad p_{11} > f + 1 \tag{2.17}$$

is suitable. The matrix P has a symmetric positive definite square root R, such that $RR = P$. Let $\zeta = R\eta$. The dynamics (2.16) becomes (time argument is dropped):

$$\dot{\zeta} - RAR^{-1}\zeta \in -R^{-1}C^T\ N_{\mathbb{R}_+}(CR^{-1}\zeta) \ \Leftrightarrow \ \begin{cases} \dot{\zeta} = RAR^{-1}z + R^{-1}C^T\lambda \\ \\ 0 \le w = CR^{-1}\zeta \perp \lambda \ge 0. \end{cases} \tag{2.18}$$

Using the symmetry of R (and thus of R^{-1}) one may use Lemma B.1 and Theorem B.2 to deduce that $R^{-1}C^T\ N_{\mathbb{R}_+}(CR^{-1}\zeta) = \partial f(\zeta)$, with $f = \psi_{\mathbb{R}_+} \circ CR^{-1} : \mathbb{R}^3 \to \mathbb{R}$. Consequently the Linear Complementarity System (2.14) is equivalent to the differential inclusion:

$$\dot{\zeta}(t) - RAR^{-1}\zeta(t) \in -\partial f(\zeta(t)). \tag{2.19}$$

Now using Definition B.8, Lemma B.1 and Theorem B.4, one deduces the following:

Lemma 2.2 *The differential inclusion in (2.19) possesses for each initial state $z(0) \in \mathrm{Dom}(\partial f)$ a unique Lipschitz continuous solution, with essentially bounded derivatives.*

[10] This property, which shall be used elsewhere in this book, is implied by the dissipativity of the system, as a consequence of the passivity Linear Matrix Inequality [218, 254].

From the fact that the system (2.5) possesses continuously differentiable solutions, while Lemma 2.2 guarantees only Lipschitz continuous solutions, we may state that:

$\rightsquigarrow$ *The relative degree between the complementarity variables in* (2.5) *and* (2.14) *influences the smoothness of the solution.*

The constraint $\zeta(0) \in \mathrm{Dom}(\partial f)$ that applies to (2.14) means that initially $z(0) \geq \xi(0)$. This implies that the spring-dashpot cannot penetrate into the wall. The last developments have been abundantly used in [22, 205, 213, 214, 215, 217, 226] to analyse various types of nonsmooth systems, relying on dissipativity, maximal monotonicity, and differential inclusions theory. The property $PB = C^T$ states in fact the passivity of the system (2.14), where $\lambda(\eta)$ and $w(\eta)$ are seen as fictitious input and output [218]. Other assemblies of linear springs, dashpots and dry friction elements have been analysed in [100, 103] and shown to yield well-posed differential inclusions whose set-valued part is a maximal monotone mapping. Our short analysis shows that there exist close links between dynamical systems with complementarity conditions, some types of differential inclusions, and some types of piecewise-linear systems. More details on the relationships between these mathematical formalisms of nonsmooth dynamical systems, may be found in [212, 438]. It is noteworthy that the manipulations made to analyze the differential inclusion (2.16) do not easily extend to nonlinear dissipative systems, like Lagrangian systems with a varying mass matrix $M(q)$, see [25] for a detailed analysis of this case.

Remark 2.5 The complementarity system has been put in the equivalent form (2.18). In particular the matrix multiplying the multiplier λ is $R^{-1}C^T$, and the matrix defining w is its transpose CR^{-1}. This allows one to recast this system in the framework of variational inequalities, for which extensions of Lyapunov stability tools exist [463]. This is quite different from systems with unilateral constraints as in (5.1) in Chap. 5. Indeed suppose that the unilateral constraints in (5.1) are of the form $f(q) = Cq \geq 0$. In the state space form of (5.1) with $x \stackrel{\Delta}{=} (q^T, \dot{q}^T)^T$, one has $w = Dx = (C \quad 0)x$. However the contact force multiplier $\lambda_{\mathrm{n},u}$ enters the state space dynamics through the matrix $B = \begin{pmatrix} 0 \\ C^T \end{pmatrix}$. Clearly $B^T \neq D$. This is due to the fact that in (5.1), the relative degree between $w = f(q)$ and λ is, roughly speaking, equal to 2: two differentiations of $w(\cdot)$ are necessary to recover $\lambda(\cdot)$.

Fixed Points of (2.14)

The matrix A is singular, so that the system $\dot{\eta}(t) = A\eta(t)$ possesses an infinity of equilibria. However, the equilibrium points of the differential inclusions (2.14) and (2.18) are given as the solutions of the generalized equations (that take the form of complementarity problems, or of inclusions into normal cones):

$$\begin{cases} A\eta^\star + B\lambda^\star = 0 \\ 0 \le C\eta^\star \perp \lambda^\star \ge 0 \end{cases} \Leftrightarrow \begin{cases} PA\eta^\star + PB\lambda^\star = 0 \\ \lambda^\star \in -N_{\mathbb{R}^+}(C\eta^\star) \end{cases}$$

$$\Leftrightarrow \quad PA\eta^\star \in -C^T N_{\mathbb{R}^+}(C\eta^\star) \quad \Leftrightarrow \quad 0 \in PA\eta^\star + N_\Phi(\eta^\star) \tag{2.20}$$

$$\Leftrightarrow \quad 0 \in -RAR^{-1}\zeta^\star + \partial f(\zeta^\star) \quad \Leftrightarrow \quad \begin{cases} 0 \in RAR^{-1}\zeta^\star + R^{-1}C^T\lambda^\star \\ 0 \le CR^{-1}\zeta^\star \perp \lambda^\star \ge 0, \end{cases}$$

where $\Phi = \{y \in \mathbb{R}^3 | Cy \ge 0\}$, and $\eta^\star = (x^\star, 0, \bar{\xi}^\star)^T$. To get these equivalences we used (B.19), Theorem B.2, Definition B.7, and the fact that P is full rank together with $PB = C^T$. Generally speaking, it could happen that A is singular while the generalized equations in (2.20) possess a unique solution. Obviously in our case there is an infinity of equilibrium points, which correspond to the noncontact phase whose mass dynamics is $\ddot{x}(t) = 0$. All the points $x^\star = z^\star - l > 0$ and $\bar{\xi}^\star = 0$ satisfy the generalized equation (2.20) with $\lambda^\star = 0$. We may modify the dynamics by either adding a constant external force F_{ext} acting on the mass, or with a feedback $u = -k_p x - k_v \dot{x}, k_p > 0, k_v > 0$. The first modification modifies the system in (2.14) as $\dot{\eta}(t) = A\eta(t) + B\lambda(t) + EF_{ext}$, with $E = (0\ \frac{1}{m}\ 0)^T$. Then if $F_{ext} < 0$ one finds that the only equilibrium is $\lambda^\star = -F_{ext}$, $\bar{\xi}^\star = \frac{F_{ext}}{k} = x^\star$ (the equilibrium belongs to the contact phase, the spring being compressed). If $F_{ext} > 0$ there is no equilibrium (the mass moves to the left). The second one modifies A to $\tilde{A} = \begin{pmatrix} 0 & 1 & 0 \\ \frac{-k_p}{m} & \frac{-k_v}{m} & 0 \\ 0 & 0 & -\frac{k}{f} \end{pmatrix}$ which is full rank. One can check that the only equilibrium is given by $x^\star = \bar{\xi}^\star = 0$ and $\lambda^\star = 0$, that corresponds to a degenerate solution of the generalized equations in (2.20).

Dissipativity Properties

It is easy to check that $PA + A^T P$ with P in (2.17) is not definite. Hence the triplet (A, B, C) is not dissipative, though $PB = C^T$.

$\rightsquigarrow$ *It is noteworthy that we are not verifying the dissipativity of a simple double integrator with PD feedback $m\ddot{x} + k_v\dot{x} + k_p x = u$, which is dissipative with supply rate $\langle u, \dot{z}\rangle$. The whole switching, complementarity system is studied.*

Let us assume that (i) $m > 1 + f$, or (ii) $m < 1 - \frac{f}{m}$. Then one can show that there exists (i) large enough k_p for fixed bounded k_v, or (ii) large enough k_v for fixed bounded k_p, such that $P\tilde{A} + \tilde{A}^T P$ is negative definite. Hence under such conditions on the gains, the system $(\tilde{A}, B, C)$ is dissipative with the supply rate $\langle w, \lambda\rangle$, i.e., it is passive. It has the storage function $V(\eta) = \frac{1}{2}\eta^T P\eta$, and due to the negative definiteness of $P\tilde{A} + \tilde{A}^T P$, the equilibrium point $x^\star = \bar{\xi}^\star = 0$ is globally, uniformly

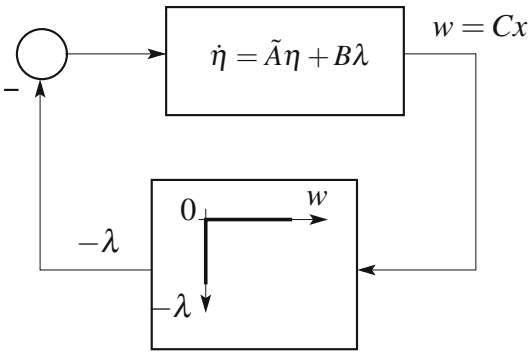

Fig. 2.2 Linear complementarity system: Lur'e set-valued system

asymptotically stable in the sense of Lyapunov. The dissipation equality is satisfied along trajectories

$$\underbrace{V(\eta(t_1))}_{\text{Energy at } t_1} - \underbrace{V(\eta(t_0))}_{\text{Energy at } t_0} = \underbrace{\int_{t_0}^{t_1} w(s)\lambda(s)ds}_{\text{Injected energy on } [t_0,t_1]} + \underbrace{\int_{t_0}^{t_1} \eta(s)^T Q\eta(s)ds}_{\text{Dissipated energy on } [t_0,t_1]}, \tag{2.21}$$

with $Q = P\tilde{A} + \tilde{A}^T P < 0$, and for any $t_0 \leq t_1$. The LCS in (2.14) with the new state matrix $\tilde{A}$ thus has the negative feedback interconnection structure as in Fig. 2.2, and may be interpreted as a Lur'e system with set-valued nonlinearity, where the dynamics is dissipative while the set-valued static nonlinearity is maximal monotone.

2.2 Viscoelastic Contact Models and Restitution Coefficients

2.2.1 Linear Spring-Dashpot

The linear spring-dashpot model has serious flaws: discontinuity in the viscous friction term for nonzero approach velocity [522] producing discontinuous acceleration, possible negative contact force (see Remark 2.3), and an equivalent restitution coefficient $e_n = \beta$ in (2.10), (2.11) or (2.12), that does not depend on the initial impact velocity. All experiments show that the colliding velocity strongly influences the restitution coefficient, that may vary from 0.9 for approach velocities $\approx$ 0.2 m/s, to less than 0.5 for velocities $\approx$ 3–5 m/s (SUJ2 steel[11] sphere/sphere impact [857]), 440c grade 100 wear resistant stainless steel sphere hitting a stainless steel puck with no hardening effects [180]. Figures 165 and 166 in [469] indicate a decrease of the restitution coefficient from 0.9 to 0.2 for lead sphere/sphere impacts, for approach

[11] Steel used for journal bearing, Japanese Industrial Standards.

velocities varyng between 0.1 and 1.6 m/s. In fact the model of Fig. 2.1 is often too simplistic to reproduce experimental results, and has therefore little prediction capabilities.

In [999] the spring-dashpot model as in Sect. 2.1.3 is used to calculate the optimal f and k that minimize the maximum value of the interaction force, given the maximum deformation. Notice that the experimental determination of the contact force represents in itself a topic of research [360, 361, 537, 713, 811]. This is typically an inverse problem in which one knows the output (displacement, velocity, strain) and the structure dynamics (a transfer function for instance [713]) and tries to compute the input (the contact force). A simple experiment allowing one to observe the shape of the curve force versus time is described in [72] for educational purpose. In [150] a nonlinear spring action $k(x)$ is used. The model is validated experimentally for low impact velocities ($\leq$ 8 m/s) of a solid cylindrical mass with blocks of polystyrene aggregate concrete. The maximum force during an impact process between two flexible bodies and using a linear spring-dashpot is calculated in [633]. Comparisons are made with experimental results using various materials. One possibility is to combine the rigid body approach (that provides one with pre and post-impact velocities and percussion) with a suitably chosen compliant model of contact/impact [1]: the compliant model is identified with the supplied data and then used to calculate the force history. Comparisons with calculations of the whole motion with methods using compliant models show good reliability of such procedure. A similar method has been used in [1122] to compare the results obtained from integration with a finite-element code and those of a rigid body approach (namely Darboux-Keller's shock dynamics, see Chap. 4).

The calculation of restitution coefficients has been considered in the mechanical engineering literature for various types of spring-dashpot models. For instance the authors in [1298] calculate e_{n} for a one degree-of-freedom system composed of a mass related to the ground by a spring of stiffness k, and striking in a compliant obstacle composed of a sprink k_1 and a damping coefficient f. Then it is found that $e_{\mathrm{n}} \stackrel{\Delta}{=} \frac{\dot{x}(t_f)}{\dot{x}(t_0)} = \exp\left(\frac{\xi\pi}{\sqrt{1-\xi^2}}\right)$, where $\xi = \frac{f}{\sqrt{(k+k_1)m}}$ (compare with (2.12)). The model of Zener consists of the linear spring-dashpot with stiffness k_1, mounted in series with another spring with stiffness k_2, see Fig. 2.3b. When $\frac{k_1}{k_1+k_2} \ll 1$, this gives the restitution coefficient:

$$e_{\mathrm{n}} = \exp\left(\left(-\frac{\alpha}{\sqrt{1-\alpha^2}} + \eta\ f_1(\alpha)\right)\left(\arctan\left(\frac{2\alpha\sqrt{1-\alpha^2}}{2\alpha^2-1}\right) + \eta\ f_2(\alpha)\right)\right), \tag{2.22}$$

with: $\alpha = \frac{k_2 f}{2(k_1+k_2)m\omega_0}$, $\omega_0 = \sqrt{\frac{k_1 k_2}{m(k_1+k_2)}}$, $\eta = \frac{k_1}{k_1+k_2}$, $f_1(\alpha) = \alpha - \frac{\alpha^3}{2} + \mathscr{O}(\alpha^5)$, $f_2(\alpha) = 2\alpha - 3\alpha^2 + \mathscr{O}(\alpha^5)$. The model of Maxwell consists of a linear spring and a linear damper mounted in series. The contact force and the indentation satisfy $\dot{\xi} = \frac{\dot{F}}{k} + \frac{F}{f}$. This model lacks of physical meaning as far as Solid Mechanics is

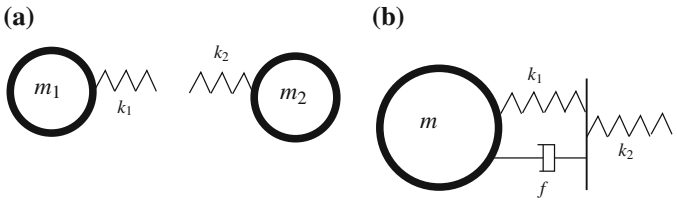

Fig. 2.3 Hodgkinson's and Zener's models

considered, because there is no static equilibrium if a constant force is applied on the system. It seems to be suited more to fluid-like behaviors. Hodgkinson [535] considered the system in Fig. 2.3a, in order to analyse the influence of each body's stiffness on the restitution process. He proposed the formula for composite restitution of coefficient $e_{\mathrm{n},12} = \frac{k_2 e_{\mathrm{n},1} + k_1 e_{\mathrm{n},2}}{k_1 + k_2}$, where $e_{\mathrm{n},1}$ and $e_{\mathrm{n},2}$ are the coefficients obtained for pairs of identical material masses.[12] Though this composite coefficient may be fitted with experiments, it may be energetically inconsistent [313, 1157]. An energetically consistent expression is $e^2_{\mathrm{n},12} = \frac{k_2 e^2_{\mathrm{n},1} + k_1 e^2_{\mathrm{n},2}}{k_1 + k_2}$ [294].

It has been argued [364, 555] that spring-dashpot models for the contacting surfaces are well-suited, because the energy-loss at impacts is associated primarily with damping rather than micro-plastic deformation or permanent strain: this is wrong if the impact velocity is such that plastification occurs. It is pointed out in [1295] after numerical and experimental investigations on impacts of a flexible arm against a rigid obstacle, that although a spring-dashpot and a more sophisticated Hertzian-like model with additional plastic effects provide similar results, the spring-dashpot parameters are more difficult to identify: this is indeed a major drawback of these models.

2.2.2 *Nonlinear Elasticity and Viscous Friction: Simon-Hunt-Crossley and Kuwabara-Kono Dissipations*

Let us remind that Hertz' contact theory yields for sphere/sphere contact an elastic force/indentation relation

$$F = \frac{4}{3} E^\star \sqrt{R} x^{\frac{3}{2}}, \tag{2.23}$$

with $\frac{1}{R} = \frac{1}{R_1} + \frac{1}{R_2}$, $\frac{1}{E^\star} = \frac{1-\nu_1^2}{E_1} + \frac{1-\nu_2^2}{E_2}$, where R_1 and R_2 are the spheres radii, E_1 and E_2 their Young elasticity modulii, ν_1 and ν_2 their Poisson's ratios (see Sect. 4.2.1.1 for more details on Hertz' contact theory). This provides an equivalent stiffness.

[12] In fact, Hodgkinson considered sphere/sphere impacts under Hertz' elasticity, which we simplify here to particle/particle impacts.

Hunt and Crossley [555] proposed a unilateral nonlinear spring-dashpot model of the form:

$$m\ddot{x}(t) = -\gamma x(t)^p \dot{x}(t) - kx(t)^p = -x(t)^p(\gamma \dot{x}(t) + k), \tag{2.24}$$

which we choose to apply during contact phases $x(t) \leq 0$,[13] where γ represents a damping parameter,[14] k is a stiffness parameter, and p is an exponent whose choice is left to the designer ($p = \frac{3}{2}$ is Hertz' elasticity, in which case $k = K_h$ in (2.23)). If we consider bilateral contact then we have to write $\gamma|x(t)|^p\dot{x}(t)$ to guarantee that this term has a meaning for any p. This model is an extension of the model proposed in [1113, Eq. (5)] who wrote it for $p = \frac{3}{2}$ and $\gamma = kf$ for some damping coefficient f, using experimental data in [196]: *The Hunt-Crossley model should thus better be called the Simon-Hunt-Crossley model*, since authors in sports science speak of the Simon's model [492, p. 253]. It has been also proposed in [1228].[15] One sees that the factor x^p in the damping term allows to pass continuously from the free to the contact motion. Let $\gamma = \frac{3}{2}\alpha k$. The model in (2.24) yields $e_\mathrm{n} \approx 1 - \alpha|\dot{x}(t_0)|$ (see [802] for a rigorous proof), with $\alpha \in [0.08, 0.32]$ s/m for steel, bronze or ivory bodies [555].[16] Various viscous friction terms may be assigned to the model by changing γ, hence changing the equivalent coefficient of restitution e_n: $\gamma = \frac{6(1-e_\mathrm{n})}{[(2e_\mathrm{n}-1)^2+3]}\frac{k}{|\dot{x}(t_0)|}$ [522], $\gamma = \frac{3}{4}\alpha k$ [716], $\gamma = \frac{3k(1-e_\mathrm{n}^2)}{4|\dot{x}(t_0)|}$ [704], $\gamma = \frac{3(1-e_\mathrm{n})}{2e_\mathrm{n}|\dot{x}(t_0)|}$ [545], $\gamma = \frac{8(1-e_\mathrm{n})}{5e_\mathrm{n}|\dot{x}(t_0)|}$ [403], $\gamma = \frac{3(1-e_\mathrm{n})}{2|\dot{x}(t_0)|}$ [555], an implicit definition[17]: $k \ln\left(\frac{\gamma|\dot{x}(t_0)|+k}{-\gamma(1-\alpha\dot{x}(t_0))|\dot{x}(t_0)|+k}\right) - 2\gamma|\dot{x}(t_0)| + \alpha\gamma\dot{x}(t_0)^2 = 0$ [470, 1323]. The coefficient α is an empirical parameter that may be obtained by fitting with experiments from the formula $e_\mathrm{n} \approx 1 - \alpha\dot{x}(t_0)$. In practice one estimates e_n via experiments, and deduces γ as in the above expressions, therefore obtaining the right spring-dashpot model. Those nonlinear spring-dashpot models typically have the force/indentation responses shown on Fig. 2.4a [442, 471, 602, 705, 802], while the linear ones typically have the response shown on Fig. 2.4b [12]. The dashed areas represent the dissipated energy during the collision process. A comparative study of all these Simon-Hunt-Crossley models is done in [38]. It follows from [38, Figs. 3, 4, 6, 7, 8, 9] that the contact force/indentation, indentation velocity/indentation displacement, and force/time diagrams show little variations from one model to the other (but the discrepancy with experimental data taken from [1324] increases if the pre-impact velocity increases). All the above models have a dissipation term of the form $D(x, e_\mathrm{n}, \dot{x}(t_0), \gamma, k)\dot{x}$. In [716], the expression

[13] Thus we assume implicitly that $x(t)^p$ exists, or we could just write $|x(t)|^p$.

[14] Often called the *hysteresis factor* [782]. The spring assures the compression/expansion, while the damping creates dissipation and the hysteresis shape.

[15] Notice that contrary to what is written just above [542, Eq. (1)] and could be misleading, the contact model in (2.24) with $p = \frac{3}{2}$ is not at all introduced in [1203].

[16] Such values should be checked and are given here just for the sake of providing an order of magnitude.

[17] It is unclear how the models which include the pre-impact velocity $\dot{x}(t_0)$, may be used in the context of multiple impacts, where some of the contact points are lasting before the collision.

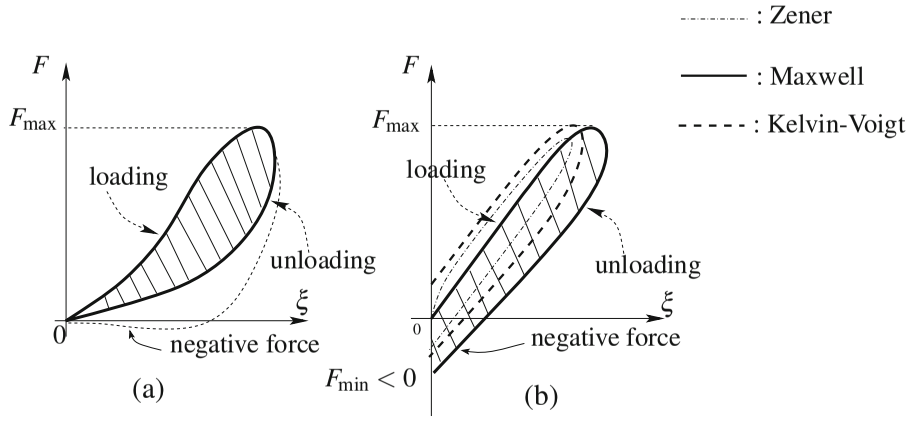

Fig. 2.4 Typical force/indentation responses for nonlinear (**a**) and linear (**b**) spring-dashpots (the abscissa is a generic indentation, or spring deformation, chosen nonnegative)

$D(x, e_\mathrm{n}, \gamma, k) = 2m\sqrt{\frac{k}{m}}\sqrt{\frac{\ln(e_\mathrm{n})^2}{\ln(e_\mathrm{n})^2+\pi^2}}\frac{x+|x|}{2x}\exp\left(\{(x-\varepsilon)-|x-\varepsilon|\}\frac{Q}{\varepsilon}\right)$ is proposed, where Q is a parameter, $0 \leq \varepsilon \leq x_{\max}$, and the contact force $D(x, e_\mathrm{n}, m, k, \varepsilon)\dot{x}+kx^{\frac{3}{2}}$ has to remain nonnegative during the collision process.

Remark 2.6 It is noteworthy that all models with $\dot{x}(t_0)$ in the denominator, yield dynamics which are ODEs of the form $\dot{z}(t) = f(z(t), z(0))$, which is unusual. In fact this corresponds to adding one dimension to the system: $\dot{z}(t) = f(z(t), y(t))$, $\dot{y}(t) = 0$, $y(0) = z(0)$. Moreover since $\dot{x}(t_0)$ is in the denominator of the vector field, some numerical problems may arise if the initial velocity is very small (think of multiple impacts in chains of balls where some balls are at rest initially).

The Simon-Hunt-Crossley model has become popular because it has some nice *ad hoc* mathematical properties, which in fact allow one to derive the above expressions for e_n by varying γ [801, 802, 1157, 1186]. Choosing $\gamma = \frac{3}{2}\alpha k$, the dynamical equation (2.24) is $m\ddot{x}(t) + kx(t)^p(1+\frac{3}{2}\alpha\dot{x}(t)) = 0$ and it is separable as $\int_{\dot{x}(t_0)}^{\dot{x}(t_f)}\frac{\dot{x}}{1+\frac{3}{2}\alpha\dot{x}}d\dot{x} + \frac{k}{m}\int_{x(t_0)}^{x(t_f)}x^p dx = 0$. If the detachment instant is such that $x(t_f) = x(t_0)$ then the second term vanishes. It is possible to show that the maximum compression occurs at $x(t_c)$ such that $x(t_c)^{p+1} = -\frac{(p+1)|\dot{x}(t_0)|}{\gamma} + \frac{k(p+1)}{\gamma^2}\ln\left|1+\frac{\gamma|\dot{x}(t_0)|}{k}\right|$ [602]. This proves that such an assumption renders $\dot{x}(t_f)$ independent of the mass and the stiffness. Introducing the restitution coefficient e_n and integrating the right-hand term, one finds $\frac{3}{2}\alpha|\dot{x}(t_0)| - \ln(1+\frac{3}{2}\alpha|\dot{x}(t_0)|) + e_\mathrm{n}\frac{3}{2}\alpha|\dot{x}(t_0)| + \ln(1-e_\mathrm{n}\frac{3}{2}\alpha|\dot{x}(t_0)|) = 0$, which makes an implicit equation for e_n. In the same vein, Chatterjee [274] computes that for $p = 1$ in (2.24) (a linear spring and a nonlinear dashpot) one obtains $-e_\mathrm{n} - \frac{1}{a}\ln(1-ae_\mathrm{n}) = 1 - \frac{1}{a}\ln(1+a)$, where a is a parameter that depends on m, f, k. The separation property is used in [1186], who noticed that the restitution coefficient does not depend on the elasticity coefficient, in case one takes it equal to kx^n with $n \neq p$ and the viscous friction force is $-\alpha x^n|\dot{x}|^q$ for some q and a parameter α. Then, one obtains the implicit equation for e_n: $\ln\left(\frac{1+\xi}{1-e_\mathrm{n}^q\xi}\right) = \sum_{j=1}^{\frac{2}{q}-1}\left((-1)^{j-1}\frac{\xi^j}{j} + \frac{(e_\mathrm{n}^q\xi)^j}{j}\right)$, with $\xi = \frac{\alpha}{k}|\dot{x}(t_0)|^q$ and $e_\mathrm{n}^q\xi < 1$. The parameters q and α have to be fitted from experiments. In case $q = 1$, the implicit equation reduces to $\ln\left(\frac{1+\xi}{1-e_\mathrm{n}\xi}\right) = (1+e_\mathrm{n})\xi$. This is extended in [373], who consider an elasticity force $f(x)$, $f(0) = 0$, $f(\cdot)$ increasing, a damping force $\gamma f(x)\dot{x}$, and prove that the CoR satisfies the transcendental equation $\gamma\dot{x}(t_0)(1+e_\mathrm{n}) - \ln(1+\gamma|\dot{x}(t_0)|) + \ln(1-e_\mathrm{n}\gamma|\dot{x}(t_0)|) = 0$. For small enough pre-impact velocities, [373] find $e_\mathrm{n} \approx 1 - \frac{2}{3}\gamma|\dot{x}(t_0)|$ which agrees with previous findings.

$\rightsquigarrow$ *These results prove that in the presence of specific damping, the CoR does not depend on the elasticity properties or the material, just as in the undamped (purely elastic) case.*

Experiments with two impacting spheres are reported in [373], showing $q = \frac{1}{5}$ for lead spheres, $q = 1$ for agate, brass, and porcelain spheres. The authors of [602] derive the implicit relationship between displacement and velocity as $\frac{\gamma\dot{x}}{k} -$

$\ln\left|1+\frac{\gamma\dot{x}}{k}\right| = -\frac{\gamma^2(x(t_c)^{p+1}-x^{p+1})}{k(p+1)}$ and approximate the $\ln(\cdot)$ by its Padé approximant. Then, they compute the energetic restitution coefficient (see Sect. 4.3.6) and compare experimental and numerical results. They show that nonlinear damping is necessary to model their experimental setup.

In fact, despite it allows some dependence on the initial impact velocity and avoids tensile contact forces,[18] the Simon-Hunt-Crossley model may lack of physical foundations. It has been experimentally shown to correctly predict the shock process for spheres and plates in [509, 1228], but not for the case of cylinders and plates [317]. In [1324] more precise conclusions have been obtained from experiments with chrome-steel balls impacting steel cylindrical specimens. The measurements concern the impact force response in terms of its peak, slope during compression and expansion phases, times of maximum compression and force peak, and impact duration

- All the above variations of the Simon-Hunt-Crossley model yield the same restitution coefficient when viscous friction is small.
- They are valid for low pre-impact velocities $\dot{x}(t_0)$, for otherwise plastic deformations may occur.
- They yield excellent predictions if $e_n > 0.95$, that is nearly lossless impacts.
- Usually, the peak force for near-elastic impacts is well-predicted, however the contact duration is poorly predicted.
- If plastic deformation occurs, they yield very poor prediction capabilities.

In [442], it is noticed that taking $\gamma = \frac{1}{e_n}\frac{k}{|\dot{x}(t_0)|}$, allows to obtain a model that provides good results for $e_n \leq 0.3$. Similar arguments are used in [403] who proposes $\gamma = k\frac{8(1-e_n)}{5e_n\dot{x}(t_0)}$. As pointed out in [602] there may exist a lag between displacement and force during impacts (detachment occurs while the bodies are still deformed; maximum contact force and maximum deformation do not match in time). The Simon-Hunt-Crossley with classical detachment conditions does not incorporate this lag. Another important issue is whether or not such models may be used in a multibody multicontact framework. As pointed out in [347], the implementation of the Simon-Hunt-Crossley model in a robotic system with unknown environment requires the on-line estimation of k, γ and p. This may not be easy in general, especially if there are many contact points involving various materials with different viscoelastic properties. A survey and comparative analysis of most of these compliant contact models is done in [783], focussing mainly on the impact process.[19]

The power coefficient p in the Simon-Hunt-Crossley model seems to be the result of some empirical idea, fitted with experiments. Starting from the theory of elasticity,

[18] This is true if no external force acts on the body. As shown in [802], when the objects are separated by an external force, then Simon-Hunt-Crossley model may yield sticky contact forces, as illustrated in Fig. 2.4a.

[19] Indeed and most importantly, using such compliant models during persistent contact phases may produce spurious, unphysical oscillations of the contact force and acceleration during numerical simulations. This is visible on many numerical results presented in the literarure, e.g., systems with clearances [403, 489, 679, 941, 1179, 1226]. It may be preferable to switch to other contact models and numerical integrators outside collisions.

and extending it to viscoelastic materials, one finds the so-called Kuwabara-Kono model [197, 198, 199, 525, 691, 902]:

$$m\ddot{x}(t) = -\gamma k|x(t)|^{\frac{1}{2}}\dot{x}(t) - kx(t)^{\frac{3}{2}}, \tag{2.25}$$

for contact phases $x(t) \leq 0$, and which corresponds to choosing $|x|^{p-1}\dot{x}$ instead of $x^p\dot{x}$ in (2.24). This type of nonlinear spring-dashpot model agrees with some experimental results [407]. Unfortunately, it has not been tested in [1324] for experimental validation.

It is clear that the separability property associated with the Simon-Hunt-Crossley models, is lost with the Kuwabara-Kono's approach. Notice that the square root in the right-hand side of (2.25) renders the vector field non-Lipschitz continuous. ODEs with non-Lipschitz vector fields have specific features in general (non uniqueness of solutions, finite-time convergence to equilibria, unbounded jacobians), which should be taken into account for analysis and numerical simulation. It is in fact a little surprizing that a viscoelastic continuum yields a non Lipschtiz continuous contact force. It is also indicated in [199] that the contact force in the right-hand side of (2.25) could be replaced when $x(t) \gg \gamma\dot{x}(t)$ by $-(x(t)+\gamma\dot{x}(t))^{\frac{3}{2}}$, providing equivalently good results when compared to some experiments. The contact force in (2.25) is almost only dissipative for small indentations, since $\gamma k|x|^{\frac{1}{2}}\dot{x} + kx^{\frac{3}{2}} = \sqrt{x}(\gamma\dot{x} + kx^3) \approx \gamma\dot{x}\sqrt{x}$ at the very beginning or at the very end of the collision where velocity is much larger than indentation: *As noticed in [12 §7.1.3], this indicates that contact forces during an impact, in the Kuwabara-Kono model, always become negative during a small period before detachment occurs, while vanishing again at the detachment time (this last property is not shared by the linear spring-dashpot with the naive switching conditions which gives a detachment force with the wrong sign).* Such spurious behavior may be avoided by imposing complementarity conditions between the contact force and the distance function.

Let the dissipative force be written as $-2\frac{\sqrt{R}}{\tilde{D}}\sqrt{x}\dot{x}$, then the Kuwabara-Kono's model for the collinear collision of two spheres gives a normal restitution $e_{\mathrm{n}} \approx 1 - 1.009\frac{5}{2}\tilde{\kappa}\left(\frac{|\dot{x}(t_0)|}{\kappa m^2}\right)^{\frac{1}{5}}$, where m is the effective mass, $\kappa = \frac{4}{5D}\sqrt{R}$, $\frac{1}{R} = \frac{1}{R_1} + \frac{1}{R_2}$, $D = \frac{3}{4}\left(\frac{1-\nu_1}{E_1} + \frac{1-\nu_2}{E_2}\right) = \frac{3}{4}\frac{1}{E^*}$, $\tilde{\kappa} = \frac{4}{5\tilde{D}}\sqrt{R}$, E_i are Young's moduli, ν_i are Poisson's ratios, $\tilde{D}$ is a viscosity parameter to be measured [508]. The impact duration is estimated as $t_f \approx \frac{\pi R}{c}\sqrt{\ln\left(\frac{4c}{|\dot{x}(t_0)|}\right)}$, with $c = \sqrt{\frac{E^*}{\rho}}$ the compressive sound velocity and ρ the density.

The authors in [906, 1027, 1080] consider the shock of two viscoelastic spheres and a Kuwabara-Kono's model $F(x,\dot{x}) = -\rho x^{\frac{3}{2}} - \frac{3}{2}A\rho\sqrt{x}\dot{x}$, where $\rho = \frac{2E\sqrt{R}}{3(1-\nu^2)}$, $A = \frac{1}{3}\frac{(3\eta_2-\eta_1)^2}{3\eta_2+2\eta_1}\left(\frac{(1-\nu^2)(1-2\nu)}{E\nu^2}\right)$, with E the Young modulus, ν the Poisson ratio, $R = \frac{R_1R_2}{R_1+R_2}$ the effective radius of the equivalent system, η_1 and η_2 are viscous material constants relating the dissipative stress and the deformation rate tensors. This yields dynamics as in (2.25). If the end of the impact is supposed to occur at the first

instant t_1 such that $\dot{x}(t_1) = 0$, then one calculates $e_\mathrm{n} = 1 + c_1 v^{\frac{1}{5}} + c_2 |\dot{x}(t_0)|^{\frac{2}{5}} + \ldots$ for some coefficients c_1, c_2 that depend on k. If the end of the collision is the first instant t_f such that $F(t_f) = 0$, then one calculates $e_\mathrm{n} = 1 + \sum_{k=0}^{\infty} h_k v^{\frac{k}{10}}$, where $v = \dot{x}(t_0)^{\frac{4}{5}}$ and for some coefficients h_k that depend on k. The parameter γ is chosen as $\gamma = \frac{\lambda^\star \sqrt{R}}{k}$ in [70], where $\lambda^\star$ is a parameter to be fitted with experimental data. It provides a restitution coefficient that varies linearly with $\ln(|\dot{x}(t_0)|)$ (but not with $\dot{x}(t_0)$). More experimental validations seem to be necessary to confirm the allegations in [70]. The Kuwabara-Kono's model has been generalized in [386] with a damping coefficient equal to $\mu \dot{x} |x|^\alpha$, $\alpha > -1$, and results in $e_n = 1 - \frac{4}{5}\mathscr{B}[\frac{3}{2}, \frac{2}{5}(\alpha+1)]\varphi$, with $\varphi = \frac{\mu}{m}\left(\frac{5m}{4k}\right)^{\frac{2(\alpha+1)}{5}} |\dot{x}(t_0)|^{\frac{(4\alpha-1)}{5}}$, and $\mathscr{B}[\cdot,\cdot]$ is a Beta function.[20] This expression holds for $e_\mathrm{n} \lesssim 1$. Another expression that applies to the nonlinear spring-dahspot with damping term $|x|^\alpha \dot{x}$ and elasticity term x^β is $e_\mathrm{n} \approx 1 - |\dot{x}(t_0)|^{\frac{2\alpha-\beta+1}{\beta+1}}$ for small initial impact velocity $\dot{x}(t_0)$ [771]. Assemblies of spring and fractional order dashpot elements are studied in [908, 1313]: such fractional-elastic rheological models apply to polymer materials. The usual dashpot element with force $f\dot{x}$ is replaced by $f D^\alpha x$, where D^α is the fractional derivative, $\alpha \in (0, 1)$. The linear dashpot is recovered in the limit $\alpha \to 1$. The authors of [197] correct their previous results [906, 1027, 1080] and find that the Kuwabara-Kono dissipative force coefficient in case of two spheres of same viscoelastic material is equal to $\frac{\sqrt{R}}{(1-\nu)^2}[\frac{4}{3}\eta_1(1-\nu+\nu^2) + \eta_2(1-2\nu^2)]$, that is different from the above one. In fact, multibody multicontact applications will in general require some parameter estimation procedure. The form of the dissipative force, (i.e., $-\gamma x^p \dot{x}$ for some p) may be more important than the analytical value of the parameter γ, that will be fitted with experimental data for a particular system.

The Simon-Hunt-Crossley model improves the linear spring-dashpot models since it allows for nonlinear elasticity, it avoids discontinuous contact forces and usually has no spurious contact forces with wrong sign. However the dissipative contact force accounts for an equivalent viscosity of the materials in contact and has to be carefully designed. Kuwabara-Kono's model for the dissipative part of the contact force originates from elasticity theory, and produces contact forces with wrong sign before the end of the collision. It is crucial to apply such models to materials which are known to be viscoelastic in the operating conditions.

Remark 2.7 (*Hamiltonian Interpretation of Simon-Hunt-Crossley and Kuwabara-Kono Model*)] Both dynamics with the Simon-Hunt-Crossley and the Kuwabara-Kono's models, may be expressed in a dissipative Hamiltonian form. Let $\mathbf{p} \stackrel{\Delta}{=} m\dot{q}$ be the linear momentum, and the Hamiltonian is $\mathscr{H}(x, \mathbf{p}) = \frac{1}{2}\frac{\mathbf{p}^2}{m} + \frac{2}{5}kx^{\frac{5}{2}}H(x)$, with

[20] $\mathscr{B}[p, q] = 2\int_0^{\frac{\pi}{2}} \cos^{2p-1}(x)\sin^{2q-1}(x)dx$.

$H(x) = 1$ if $x \leq 0$, $H(x) = 0$ if $x \geq 0$. Both (2.25) and (2.24) with $p = \frac{3}{2}$ are rewritten equivalently as[21]:

$$\begin{pmatrix} \dot{x} \\ \dot{\mathbf{p}} \end{pmatrix} = \left[\begin{pmatrix} 0 & 1 \\ -1 & 0 \end{pmatrix} - R(x) \right] \underbrace{\begin{pmatrix} kx^{\frac{3}{2}} H(x) \\ \frac{\mathbf{p}}{m} \end{pmatrix}}_{= \frac{\partial \mathscr{H}}{\partial (x, \mathbf{p})}}, \tag{2.26}$$

with $R(x) = \begin{pmatrix} 0 & 0 \\ 0 & \gamma \sqrt{|x|} H(x) \end{pmatrix} \geq 0$ for Kuwabara-Kono, and $R(x) = \begin{pmatrix} 0 & 0 \\ 0 & \gamma x^{\frac{3}{2}} H(x) \end{pmatrix} \geq 0$ for Simon-Hunt-Crossley. Adding external force inputs, and defining a proper dissipative output, one finds a so-called *port controlled Hamiltonian system with dissipation* [218, Definition 6.37], which is dissipative in Willem's sense provided the Halmiltonian is bounded from below [218, Lemma 6.38].

A five-parameter viscoelastic model incorporating complementarity conditions has been proposed in [1287]. It is meant to improve the Simon-Hunt-Crossley model, avoiding sticky contact forces, and allowing for non zero remaining indentation. This is particularly important in view of the fact that the Simon-Hunt-Crossley model is known to overestimate the contact time, because the spring has to fully unload to get detachment, if no nonnegativity of the contact force is imposed [602]. The new model is formulated as follows:

$$\begin{cases} a(t) + \left(\frac{1}{\gamma} + \beta_1 + \beta_2 a(t) \right) \dot{a}(t) \in -\partial \psi_{\mathbb{R}^+} (\gamma (a(t) - \delta(t) |\delta(t)|^{\lambda - 1}) + \dot{a}(t)) \\ F(t) = K \left(a(t) + \left(\frac{1}{\gamma} + \beta_1 + \beta_2 a(t) \right) \dot{a}(t) \right), \end{cases} \tag{2.27}$$

with $\lambda \geq 1$, $\beta_1 \geq 0$ and $\beta_2 \geq 0$ are damping parameters, $\gamma > 0$ is a parameter, and $\delta = -x$ is the indentation (i.e., the spring's deformation). The variable $a(t)$ is an internal state. Let us remind that $\partial \psi_{\mathbb{R}^+}(\cdot)$ is the subdifferential in the sense of convex analysis, of the indicator function of $\mathbb{R}^+$ (see Appendix B). One may use the material in Sect. B.2.1 to further develop (2.27). In particular complementarity conditions are present in (2.27), since the first line of (2.27) is equivalent to:

$$0 \leq a(t) + \left(\frac{1}{\gamma} + \beta_1 + \beta_2 a(t) \right) \dot{a}(t) \perp \gamma (a(t) - \delta(t) |\delta(t)|^{\lambda - 1}) + \dot{a}(t) \geq 0, \tag{2.28}$$

[21] For instance, polymers or metals with sufficiently high temperature are known to exhibit viscoelastic behaviors.

letting $\Phi = \mathbb{R}_+$ in (B.19). Let us assume that $\frac{1}{\gamma} + \beta_1 + \beta_2 a(t) > 0$.[22] The first line in (2.27) is equivalent to (time argument is dropped):

$$\begin{aligned} \gamma(a - \delta|\delta|^{\lambda-1}) + \dot{a} + \frac{a - \left(\frac{1}{\gamma} + \beta_1 + \beta_2 a\right)\gamma(a - \delta|\delta|^{\lambda-1})}{\frac{1}{\gamma} + \beta_1 + \beta_2 a} \\ \in -\partial\psi_{\mathbb{R}^+}(\gamma(a - \delta|\delta|^{\lambda-1}) + \dot{a}), \end{aligned} \tag{2.29}$$

Using (B.20) this is equivalently rewritten as:

$$\begin{aligned} \gamma(a - \delta|\delta|^{\lambda-1}) + \dot{a} &= \text{proj}[\mathbb{R}_+; \tfrac{-\gamma a}{1+\gamma(\beta_1+\beta_2 a)} + \gamma(a - \delta|\delta|^{\lambda-1})] \\ &= \max[0; \tfrac{-\gamma a}{1+\gamma(\beta_1+\beta_2 a)} + \gamma(a - \delta|\delta|^{\lambda-1})]. \end{aligned} \tag{2.30}$$

Using the expression of $F(t)$ in (2.27) one obtains:

$$F(t) = k\frac{1 + \gamma(\beta_1 + \beta_2 a(t))}{\gamma}(z(t) + \max[0; -z(t)]), \tag{2.31}$$

with $z(t) = \frac{\gamma a(t)}{1+\gamma(\beta_1+\beta_2 a(t))} - \gamma(a(t) - \delta(t)|\delta(t)|^{\lambda-1})$. Finally one obtains:

$$F(t) = K\max(0; -\delta(t)|\delta(t)|^{\lambda-1} - \gamma(\beta_1 + \beta_2 a(t))(\delta(t)|\delta(t)|^{\lambda-1} - a(t))) \geq 0. \tag{2.32}$$

The expressions in (2.30) and (2.32) may be used to integrate the dynamics, that is a piecewise nonlinear system. The inclusion in (2.27) secures the non negativity of the contact force $F(t)$ in a similar way as (2.15) does. One may rewrite equivalently (2.32) as $F(t) = K\lambda$, with λ the unique solution of the LCP:

$$0 \leq \lambda \perp w(\lambda, \delta, a) = \lambda + \delta(t)|\delta(t)|^{\lambda-1} + \gamma(\beta_1 + \beta_2 a(t))(\delta(t)|\delta(t)|^{\lambda-1} - a(t)) \geq 0. \tag{2.33}$$

The complementarity conditions in (2.5), (2.14) and (2.33) may all be depicted as in Fig. 2.5a.

Setting $\beta_1 = 0$ and $\beta_2 = 0$ and $\lambda = \frac{3}{2}$, it follows that $F(t) = k\max[0; -\delta(t)|\delta(t)|^{\frac{1}{2}}]$, which we may rewrite as $F(t) = 0$ if $x(t) \geq 0$, $F(t) = -kx(t)|x(t)|^{\frac{1}{2}}$ if $x(t) \leq 0$ (in order to recover the conventions adopted above, one just has to set $\delta = -x$). Some comments arise: it seems from the simulations presented in [1287] that the inequality $\frac{1}{\gamma} + \beta_1 + \beta_2 a(t) > 0$ is satisfied when $a(0) = 0$; β_1 determines the residual indentation; β_2 influences the roundedness of the curves $(F(t), x(t))$ and may model the displacement/force lag[23]; while γ influences the overall shape of these curves; the internal state $a(t)$ allows for some dependence of the restitution coefficient

[22] It is not mentioned in [1287] how this condition may be guaranteed.

[23] The shape in Fig. 2.5b for large β_2 presents strong similarities with the experimental curves shown in [602].

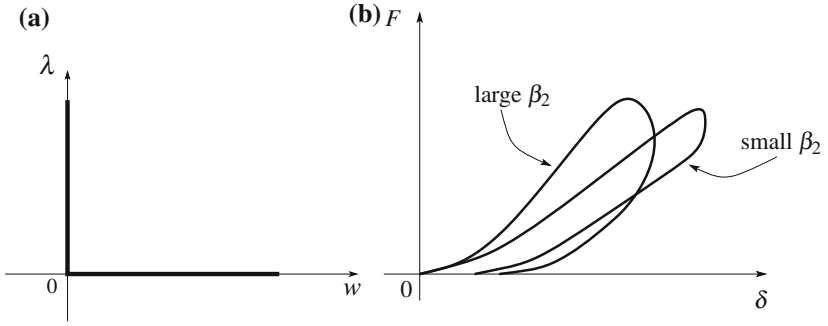

Fig. 2.5 Force/distance and force/indentation *curves*. **a** Complementarity in (2.5), (2.14) and (2.33). **b** For (2.32)

on the pre-impact velocity $\dot{x}(t_0)$. The force/indentation curves typically possess the shape as in Fig. 2.5a. The various force/indentation curves depicted in Figs. 2.4 and 2.5a, have the same global shape as experimental curves shown for instance in [312, Fig. 2], obtained from low-velocity impacts of tennis,[24] golf, baseball, plasticene, steel balls, and superball. In most of the cases, a permanent indentation exists after the shock, indicating some plastification. Vibrations seem to play a role in tennis balls collisions.

Let us end this (non exhaustive) presentation of viscoelastic contact models, by mentioning a sphere/thin plate model using the developments of Zener [1314]. Applications are in harvesting, in order to better understand the dynamics of fruits or potatoes so that clods and stones may be separated from them [426, 430].

2.2.3 Conclusions

⇝ *Most of the above models are of limited practical use in a multibody system context with many contact/impact points, mainly because it is difficult to estimate the contact parameters (even if there is only one contact). Another reason may be related to numerical issues (stability, stiff equations, constraints stabilization). It is also noteworthy that most of them use an empirical, non physical parameter that has to be fitted with experimental data.*

⇝ *Let us remind that all these models assume low velocity impact*, i.e., *local deformations only (this is sometimes called the stereomechanical impacts). Plastification effects are not taken into account. See section 4.2.1 for more details. As a consequence they are valid for very small dissipation collisions only.*

Let us tentatively classify pre-impact velocities, in a kind of "definition".

[24] High-velocity impacts of tennis balls, which are not spheres but shells, involves some buckling effects and cannot be modeled with such simple equations.

Definition 2.1 (*Pre-impact velocities*) *Very low velocity impacts* occur for pre-impact velocities $\in (0 - 100)$ cm/s. *Low-velocity impacts* occur for pre-impact velocities $\in (1 - 10)$ m/s. So-called *hypervelocity impacts* occur for pre-impact velocities $\in [1 - 10]$ km/s [40, 550, 757]. Hypervelocity impacts induce material failure, cracks, craters, debris. *High-velocity impacts* are in-between low-velocity and hypervelocity impacts, with pre-impact velocities ≈ 100 m/s. Body vibrations, temperature rise in the bodies, may not be neglected any longer.

The discrepancy between very low, and low velocities impacts, is that one may observe that $e_{\rm n}$ increases when the pre-impact velocity increases for the former, while $e_{\rm n}$ decreases as the pre-impact velocity increases for the latter. See Sect. 4.2. In nonsmooth mechanics one usually deals with low-velocity impact. However very low velocities and high velocities may be considered as well.

2.3 Viscoelastic Models with Dry Friction Elements: Viscoelasto-Plastic Models

We have focused almost uniquely on very simple assemblies of one spring and one dashpot. Many types of more complex assemblies and patterns have been proposed and analyzed in the Solid Mechanics literature, like generalized Kelvin-Voigt, generalized Maxwell, ladder, Masing models, etc. [100, 103, 104, 1219]. Some of these assemblies are made of springs, dashpots and dry friction elements which aim at modeling plasticity. A "dry friction element", also called a Saint-Venant element, produces a force of the form $F \in -F_c \mathrm{sgn}(v)$, where $\mathrm{sgn}(v) = [-1, 1]$ when $v = 0$, $\mathrm{sgn}(v) = 1$ if $v > 0$ and $\mathrm{sgn}(v) = -1$ if $v < 0$, and $F_c \geq 0$ is known as a Coulomb's force.[25] In the Systems and Control literature this is known as a relay function. Bastien et al. [100, 103, 104] proved that some of these assemblies define maximal monotone mappings. This is a useful step for both mathematical (existence and uniqueness of solutions of the dynamics with set-valued right-hand side) and physical (dissipativity of the contact model) viewpoints. We already tackled this issue in Sect. 2.1.3.4, see Fig. 2.2. Let us focus on the assembly studied in [100], known as Persoz's gephyroidal model,[26] introduced in [997] and depicted in Fig. 2.6. The dry friction elements have the force/velocity set-valued laws $G_i \in -\alpha_i \mathrm{sgn}(\dot{v}_i)$ for $i = 2, 3$ and $G_1 \in -\alpha_1 \mathrm{sgn}(\dot{u}_1)$. The linear springs have the force/displacement laws $F_i = -k_i u_i$, $i = 1, 2, 3$. In order to derive the equations governing this system, we need the following bilateral constraints: $u_0 + v_3 + u_2 = x$, $v_2 + u_3 + u_0 = x$, $u_1 + u_3 = v_3$, plus the force balance equations $G_2 + F_1 + G_1 = F_3$, $G_3 + F_3 = F_0$, $G_3 + G_1 + F_1 = F_2$, and $m\ddot{x}(t) = F_0(t) + F(t)$. There are 14 unknowns and 14 equations. Then the following is true.

[25] Coulomb's friction is introduced in more detail in Sect. 5.3.

[26] The word gephyroidal comes from the Greek "bridge".

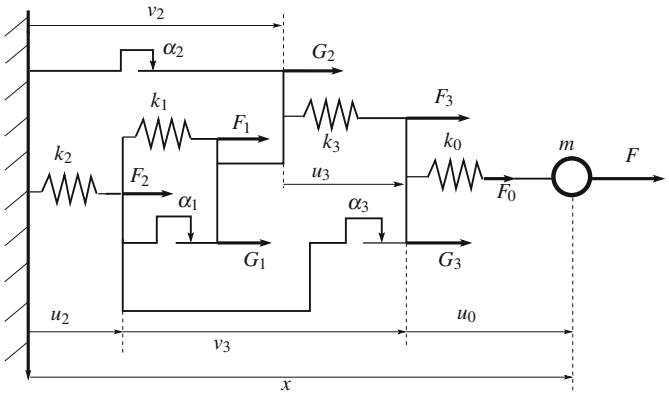

Fig. 2.6 Persoz's rheological (gephyroidal) contact model

Proposition 2.2 *[98, 100] Let* $K = \begin{pmatrix} k_0+k_2 & k_0 & -(k_0+k_2) \\ k_0 & k_0+k_3 & -(k_0+k_3) \\ -(k_0+k_2) & -(k_0+k_3) & k_0+k_1+k_2+k_3 \end{pmatrix}$, $G \triangleq \begin{pmatrix} G_2 \\ G_3 \\ G_1 \end{pmatrix}$, $\phi(G) \triangleq \sum_{i=1}^{3} \psi_{[-\alpha_i,\alpha_i]}(G_i)$, $U = (1\ 1\ -1)^T$, $E = k_0 U^T K^{-1}$, $\delta = k_0(1 - EU)$. *Let also* $k_0 = 0$ *and* $k_i > 0$, *or* $k_0 > 0$ *and at least two among* k_1, k_2, k_3 *are* > 0 ($\Leftrightarrow K = K^T \succ 0$). *Then the Persoz's gephyroidal system dynamics is given by:*

$$\begin{cases} \dot{x}(t) = y(t) \\ \dot{y}(t) = \frac{1}{m}(F(t) - \delta x(t) + EG(t)) \\ \dot{G}(t) + k_0 U y(t) \in -K\ \partial\phi(G(t)), \end{cases} \tag{2.34}$$

which is a differential inclusion of the type $\frac{dz}{dt}(t) - f(t, z(t)) \in -P\ \partial\varphi(z(t))$, $z(0) = z_0$, $P = P^T \succ 0$, *with* $\varphi(\cdot)$ *a proper convex lower semicontinuous function,* $\partial\varphi(\cdot)$ *its subdifferential, and* $P = diag(1, 1, K)$.

Apart from the elimination of some coordinates using the bilateral constraints, the proof uses some tools from convex analysis like the inversion of the dry friction laws (see Appendix B, Fig. B.4), which makes the indicator functions $\psi_{[-\alpha_i,\alpha_i]}(G_i)$ appear (that is, use is made of $x \in \text{sgn}(y) \Leftrightarrow y \in \partial\psi_{[-1,1]}(x) = N_{[-1,1]}(x)$, or the reader may also work with the function $f_4(\cdot)$ defined just above Fig. B.4). The obtained differential inclusion has a maximal monotone set-valued right-hand side, it is similar to the differential inclusion in (2.19) and its well-posedness may be shown using Theorem B.4. For this, one may perform a variable change as $x = R^{-1}z$ with $R = R^T \succ 0$ and $R^2 = P$. Thus, $\dot{x}(t) = R^{-1}\dot{z}(t) \in R^{-1}f(t, Rx(t)) - R\ \partial\varphi(Rx(t))$. Using Theorem B.2 and Lemma B.1, the result follows.

In [1286], similar assemblies called generalized Maxwell-slip friction models are proposed and analyzed for the sake of properly modeling frictional contact. Therein

the Saint-Venant element is not inserted inside the assembly structure, but at the interface between the assembly and the contact point. The Masing model with and without viscosity is depicted in Fig. 2.8a, b. The viscoelasto-plastic model of [1286] is in Fig. 2.8c. The dynamics of the viscous Masing model is given by the differential inclusion [101]:

$$\begin{cases} F(t) = kw(t) + k_0 u(t) + f\dot{u}(t) - k_0 l_0 \\ \dot{w}(t) - \dot{u}(t) \in -\partial\psi_{[-1,1]}\left(\frac{w(t)}{\eta}\right) \\ w(0) = w_0, \end{cases} \tag{2.35}$$

where $w = u_s - l, \eta = \frac{\alpha}{k}, u = u_s + u_t, u_s$ is the spring deflection, u_t is the dry friction element deflection, l and l_0 are the spring-free lengths. Once again the dry friction laws are inversed in this formulation. The existence and uniqueness of solutions for the differential inclusion in (2.35) may be proved using Theorem B.4. When $u(\cdot)$ is periodic, both viscous-free and viscous Masing's model possess a force/indentation (F, u) characteristic with hysteresis stick/slip loop as in Fig. 2.7, which is analyzed in [101]. Parameter identification is performed on a belt tensioner setup in [101].

The dynamics of the model in Fig. 2.8c is given by the differential inclusion:

$$\begin{cases} k_i a_i(t) + f_i \dot{a}_i(t) \in \alpha_i \gamma(t) \mathrm{sgn}(v(t) - \dot{a}_i(t)), \quad 1 \le i \le n \\ \dot{\gamma}(t) = \frac{g(v(t)) - \gamma(t)}{\tau_d} \\ F_c \le \gamma(0) \le F_s, \end{cases} \tag{2.36}$$

where each dry friction element produces the force $\alpha_i \gamma(t)\mathrm{sgn}(v(t) - \dot{a}_i(t))$, $\tau_d > 0$, and $g(v) = F_c + (F_s - F_c)\exp\left(-\left|\frac{v}{v_s}\right|^{\beta}\right)$ models the Stribeck effect during sliding motions, where $0 < F_c < F_s$ so that $g(v) > 0$. This model captures frictional lag with the added state variable $\gamma(\cdot)$. Starting the analysis of (2.36), it is noteworthy that the first line involves $\dot{a}_i(t)$ in both sides of the inclusion.

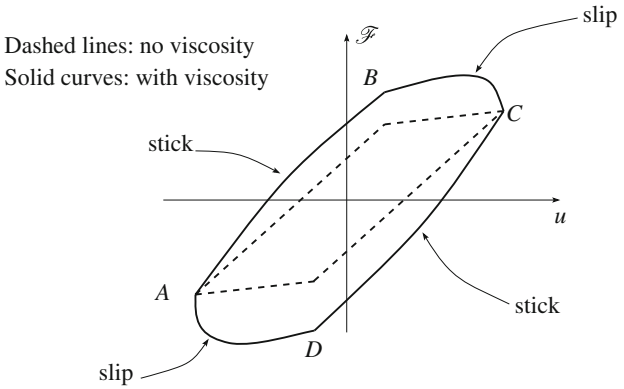

Fig. 2.7 Hysteresis loops in Masing's models with and without viscosity

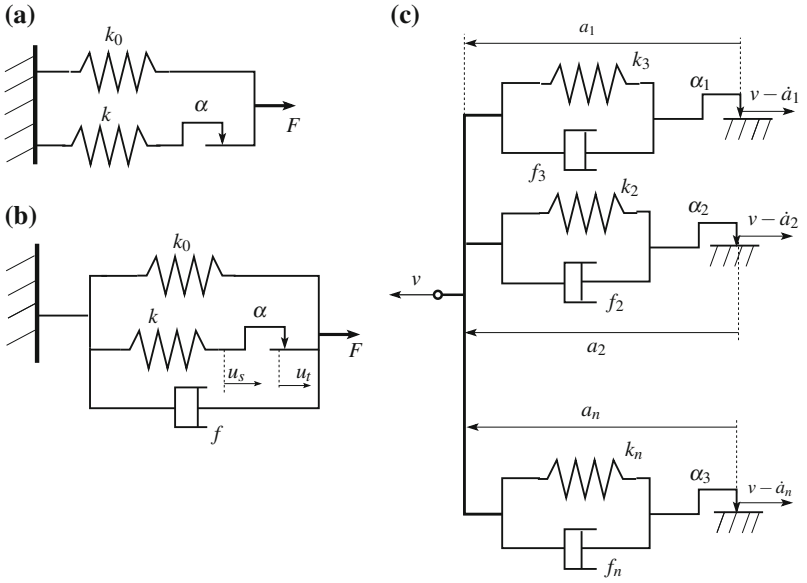

Fig. 2.8 Masing and viscoelasto-plastic contact models

Inverting this inclusion following the tools in Appendix B (see (B.15) and (B.16)) we obtain $-v(t)+\dot{a}_i(t) \in -N_{[-1,1]}\left(\frac{k_i a_i(t)+f_i \dot{a}_i(t)}{\alpha_i \gamma(t)}\right)$. Using (B.20) and the fact that $\gamma(t) > 0$ we infer that $f_i \dot{a}_i(t) + k_i a_{(}t) = \alpha_i \gamma(t)\text{proj}\left([-1,1]; \frac{f_i v(t)+a_i(t)}{\alpha_i \gamma(t)}\right)$. The projection operator is Lipschitz continuous, and one finds by inspection that it may be rewritten using a saturation function sat$(\cdot)$, which is familiar to the Control scientific community. The friction contact force is therefore found to satisfy $F = \sum_{i=1}^{n}(k_i a_i + f_i \dot{a}_i) = \sum_{i=1}^{n} \text{sat}(\alpha_i \gamma(t), k_i a_i(t) + f_i v(t))$. Here sat$(z, x) = 1$ if $x \geq z$, -1 if $x \leq -z$, z if $|x| \leq z$, $z \geq 0$. It is proved in [1286] that this model guarantees that the nonviscous part of the frictional force is bounded, the friction force is time-continuous, and most importantly it is dissipative with storage function $V(a_i) = \sum_{i=1}^{n} \frac{k_i}{2} a_i^2$, and supply rate vF. It is also free of spurious drifting phenomena during sticking modes. Further studies on the same type of assemblies may be found in [1284, 1285]. They are used for energy transfer purpose in two-degree-of-freedom systems in [1077]. All these models, which are encapsulated into differential inclusions with maximal monotone set-valued right-hand side, can be discretized with implicit Euler methods as described in Sect. 5.7.3.4, whose convergence is analyzed in [97, 102].

Remark 2.8 (*Saturation from relay*) As pointed out in [664], the feedback system in Fig. 2.9 realizes a saturation function. This is easily proved using conjugacy, inversion (Definition B.11, (B.16) and Fig. B.4), and (B.20). Let all vari-

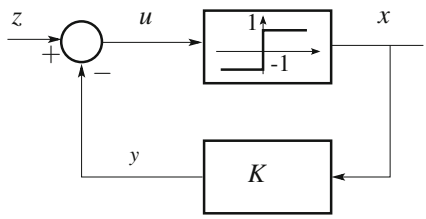

Fig. 2.9 Realization of saturation via set-valued relay

ables be $n-$dimensional, and $\mathrm{sgn}(u) \stackrel{\Delta}{=} (\mathrm{sgn}(u_1), \mathrm{sgn}(u_2), \ldots, \mathrm{sgn}(u_n))^T$.[27] We have $x \in \mathrm{sgn}(u)$ with $u = z - y$ and $y = Kx$, thus $x \in \mathrm{sgn}(z - Kx) \Leftrightarrow Kx - z \in -N_{[-1,1]^n}(x) \stackrel{K=K^T\succ 0}{\Longleftrightarrow} x = \mathrm{proj}_K([-1, 1]^n; K^{-1}z)$, showing that x is a Lipschitz continuous function of z. Let $K = 1$ and $n = 1$, then $x = \mathrm{proj}([-1, 1]; z)$ which is the classical saturation function $\mathrm{sat}(z)$.

2.3.1 Conclusions and Further Reading

The complementarity conditions and associated convex analysis results, prove to be quite powerful tools to enhance the basic spring-dashpot model. It allows the designer to guarantee some fundamental properties of the assemblies like dissipativity, well-posedness, maximal monotonicity using results on complementarity dynamical systems, or differential inclusions with maximal monotone right-hand side (see (2.5), (2.16), (2.27), (2.34), (2.35) and (2.36)). This has important consequences for Mathematical and Numerical Analysis, as well as for Control. Many other assemblies of linear springs and Saint-Venant elements are studied in [103]. Such rheological models are introduced to represent elastoplastic behaviors of materials. The main issue after their dissipativity is to determine whether these assemblies are well-posed, i.e., do they yield a unique contact force and do they define an operator which yields a well-posed dynamical system. The differential inclusion framework adopted in [98, 99, 100, 101, 103] and in [1284, 1285, 1286] is very powerful. A tentative classification of rheological models made of assemblies of linear springs, linear dashpots, and dry friction elements, is made in [103, Table I] from the structure of the convex function $\varphi(\cdot)$ as in Proposition 2.2. It is noteworthy that the analysis that yields Proposition 2.2 as well as the dynamics in (2.35) does not take into account the unilateral feature of the contact: a complementarity condition that rules detachment from the constraint has to be added. It should in particular guarantee $F(t) \geq 0$. Assemblies of spring and fractional order dashpot elements are studied in [908, 1313]: such fractional-elastic rheological models apply to polymer materials. It is noteworthy that various types of assemblies quite similar to the above ones may be used for

[27] Such a definition is logical if one thinks of $\mathrm{sgn}(\cdot)$ as the subdifferential of $f(u) = |u_1| + |u_2| + \ldots + |u_n|$.

vibration absorbers design [545]. The various viscoelastic models reviewed above, show an hysteretic force/indentation law. However the hysteresis phenomenon may be velocity-independent and due only to Coulomb's friction effects, like in felt where the interacting fibers rub each other [817].

2.4 Penalizing Functions in Mathematical Analysis

The goal of the studies summarized below, is to prove that some sequence of second order differential equations $\mathscr{P}_{n,Q}: \ddot{q}_n(t) + F_n(q_n(t), \dot{q}_n(t)) = Q(t, q_n(t), \dot{q}_n(t))$, that is considered to represent the physical model of a body colliding with a compliant constraint, converges towards a limit problem in which the constraints are rigid, i.e., unilateral. By convergence it is meant that solutions $q_n(\cdot)$ converge as $n \to +\infty$. The functions $F_n(\cdot)$ are called penalizing functions and aim at modeling the elasticity and the viscous damping of the body's surface. In all the results that follow, it is assumed a constraint surface of codimension 1, i.e., $f(q) \in \mathbb{R}$, and satisfying the basic requirements of Definition 1.8. The case of multiple unilateral contacts is more tricky, see Chaps. 5 and 6.

Remark 2.9 The dynamical systems that are studied as the limit of a sequence of compliant, or penalized problems, belong to the class of Measure Differential Inclusions: indeed they possess a set-valued right-hand side (due to the unilateral constraints and complementarity conditions), moreover they involve velocity discontinuities at impacts, hence acceleration and contact force are Dirac measures at impact times. Typically, a system like in Example 1.6 with fixed $y(t) = y_0$ can be analyzed with the following tools, showing that the inextensible cable is really a limit of stiff cables.

2.4.1 The Elastic Rebound Case

The basic assumption is that energy is conserved at the impacts. The considered problem is the following and deals with a one-degree-of-freedom system:

Problem 2.1 [260, 261] A locally Lipschitz function $q(\cdot)$ defined on $[0, T]$ is a solution of the one-dimensional rebound problem $\mathscr{P}_Q$ if:

(**a**) $q(t) \leq 0$ on $[0, T]$.
(**b**) $\langle \ddot{q} - Q, \varphi \rangle \leq 0$ for all $\varphi \in \mathscr{D}_{[0,T]}$, $\varphi \geq 0$, $Q \in L_1([0, T])$.
(**c**) If $q < 0$ then $\ddot{q} - Q = 0$ in the distributional sense.
(**d**) $\forall t \in [0, T]$, $\dot{q}(t^+)$ and $\dot{q}(t^-)$ exist, $\dot{q}(0^+)$ and $\dot{q}(0^-)$ exist, $\frac{1}{2}[\dot{q}(t^+)]^2 - \frac{1}{2}[\dot{q}(0^+)]^2 = \int_0^t Q(\tau)\dot{q}(\tau)d\tau$, and the equality holds also for $\dot{q}(t^-)$.

The initial data are naturally assumed to be admissible, in particular if $q(0) = 0$ then $\dot{q}(0^+) \leq 0$, in order not to violate the constraint. (**a**) is the unilateral constraint

condition; (**b**) means that the (impulsive) interaction force at impacts is a negative measure, i.e., there is a measure μ such that $\ddot{q} - Q = \mu$ and $\langle \mu, \varphi \rangle$ is either negative or zero if $q < 0$ as stated by (**c**), which merely means that the smooth dynamical equations are verified (in Example 1.1 we have $\mu = p_k \delta_{t_k}$ and $p_k = -2m\dot{q}(t_k^-) < 0$ when the shock is lossless. Adopting the notations of Chap. 1, we get $\ddot{q} = \{\ddot{q}\} + \sum \sigma_{\dot{q}_k} \delta_{t_k}$, so that (**b**) and (**c**) becomes $\sigma_{\dot{q}}(t_k) < 0$ and $\{\ddot{q}\} = Q$). (**d**) is a dissipation equality which rules the energetical behavior of the system (including at impacts), and the supply rate is the product $Q\dot{q}$, where Q is an external force applied on the system.

One therefore realizes that except for trivial cases ($Q \geq 0$ and $q(0^-) = 0$ or $Q \leq 0$) μ is atomic with atoms the zeros of q. The first aim of these works is to prove the existence of a solution to $\mathscr{P}_Q$. Existence is studied in [260] by choosing in $\mathscr{P}_{n,Q}$ a continuous penalizing function $F_n(q_n(t))$ such that the contact force satisfies $F_n(\zeta) = 0$ if $\zeta \leq 0$, $F_n(\zeta) > 0$ for $\zeta > 0$, $F_n \to +\infty$ on any compact interval of $(0, +\infty)$, and $\lim_{\zeta \to 0^+} \lim_{n \to +\infty} \frac{F_n(\zeta)}{\alpha_n(\zeta)} = +\infty$, with $\alpha_n(\zeta) = \int_0^\zeta F_n(\tau) d\tau$. It is easy to verify that the spring-like environment studied in the preceding part of this chapter fits within this framework (thus clearly such penalizing functions aim at modeling a spring, but other examples with no clear physical meaning may be found, see [260]). Theorem 1 in [260] states that if $q_n(\cdot)$ is a solution to $\mathscr{P}_{n,Q}$ that tends uniformly to a function $q(\cdot)$, then $q(\cdot)$ is a solution of $\mathscr{P}_Q$, and that there exists at least one solution to $\mathscr{P}_Q$ for each initial data, which is the uniform limit of some sequence $\{q_n(\cdot)\}$.

Buttazzo and Percivale [241, 242, 989, 990] considered the same problem $\mathscr{P}$ as Problem 2.1, however for n-degree-of-freedom systems. Similar results as in [260, 261] are obtained in [241] (a paper written between the other two) for the one-dimensional case. Condition (**c**) is stated in [241] (as well as in [242, 989, 990] for the higher-dimensional case) as $\text{supp}(\ddot{q} - Q) \subseteq \{t \in [0, T] | q(t) = 0\}$, *i.e.,* the support of the distribution $\ddot{q} - Q$ is contained in the set of zeros of $q(t)$ when the particle attains the constraint. The results in [242, 989, 990] incorporate a variational formulation of the elastic bounce problem. We shall come back in more details on these articles in Chap. 3, Problem 3.1.

2.4.2 The Case with Dissipation (Linear Viscous Friction)

Let us describe now the work in [969], which considers a rebound problem with possible dissipative collisions. The problem is the following:

Problem 2.2 (*Constant Mass Matrix* [969]) Let $F : [0, T] \times \mathbb{R}^n \times \mathbb{R}^n \to \mathbb{R}^n$ be continuous in t, q, $\dot{q}$ and Lipschitz in q, $\dot{q}$, uniformly with respect to q, Φ be a closed convex domain $\subset \mathbb{R}^n$, with nonempty interior and with smooth boundary $\text{bd}(\Phi)$. Then, $q : [0, T] \to \mathbb{R}^n$ is a solution of the problem $\mathscr{P}_F$: $\ddot{q} + \partial \psi_\Phi(q) \ni F(t, q, \dot{q})$, $\dot{q}_{\text{n}}(t_k^+) = -e_{\text{n}} \dot{q}_{\text{n}}(t_k^-)$ when $q(t_k) \in \text{bd}(\Phi)$, where the subscript $_{\text{n}}$ denotes the component normal to $\text{bd}(\Phi)$, $e_{\text{n}} \in (0, 1]$, if $q(\cdot)$ fulfills the following:

(**a**) $q(\cdot)$ is Lipschitz continuous and $\dot{q}$ is of bounded variation.
(**b**) $q(t) \in \Phi$ for all $t \in [0, T]$.
(**c**) for any continuous function $v : [0, T] \to \Phi$, $\langle v - q, F - \ddot{q} \rangle \leq 0$.
(**d**) the initial data satisfy $\dot{q}_{\mathrm{n}}(0^+) = -e_{\mathrm{n}}\dot{q}_{\mathrm{n}}(0^-)$ when $\dot{q}(0^-)$ points outwards Φ.

Condition **(c)** concerns the reaction on the constraint boundary $\mathrm{bd}(\Phi)$. When $q \in \mathrm{Int}(\Phi)$ then the subdifferential is reduced to $\{0\}$ and the inequality is trivially satisfied. When $q \in \mathrm{bd}(\Phi)$, there is a reaction $\lambda = \ddot{q} - F$ acting on the particle to maintain it inside Φ (mathematically speaking λ is a measure). Hence the inequality in **(c)** can be rewritten as $\langle v - q, \lambda \rangle \geq 0$. Notice that v is a function that takes its values in Φ. This permits to assert that **(c)** implies that $-\sigma_{\dot{q}}(t_k) \in T_{\Phi}(q(t_k))$ (see Definition B.2 for the tangent cone to a closed convex set). The inequality **(c)** means that $(F - \ddot{q})$ is a subgradient of the indicator function $\psi_{\Phi}(\cdot)$, i.e., $\psi_{\Phi}(v) - \psi_{\Phi}(q) \geq (F - \ddot{q})(v - q)$ for all $v \in \mathbb{R}$. Thus $(F - \ddot{q})$ is a vector that belongs to the subdifferential $\partial\psi_{\Phi}(q)$, by definition. See Appendix B for more details.

Example 2.1 Let us consider $q(t) \in \Phi = [a, b]$, $b > a$ real numbers, for all $t \in [0, T]$. Then the following formulations are equivalent (impacts are disregarded):

$$\begin{cases} \ddot{q} = F(t, q, \dot{q}) + \mu \ \text{ in the sense of distributions,} \\ q \in C^0\left([T, T']; \Phi\right), \\ \langle \mu, v - u \rangle \leq 0, \forall\, v \in C^0\left([T, T']; \Phi\right), \ \text{or equivalently :} \ \ \mathrm{supp}(\mu) \subset \{t | u(t) \in \mathrm{bd}(\Phi)\}, \\ \mu \geq 0 \text{ on } \{t | u(t) = a\}, \mu \leq 0 \text{ on } \{t | u(t) = b\}. \end{cases} \tag{2.37}$$

or:

$$\ddot{q}(t) + \partial\psi_{\Phi}(q(t)) \ni F(t, q(t), \dot{q}(t)), \tag{2.38}$$

where (see Appendix B) $\partial\psi_{\Phi}(q) = N_{\Phi}(q) = \begin{cases} \{0\} \text{ if } a < q < b \\ \mathbb{R}^+ \text{ if } q = b \\ \mathbb{R}^- \text{ if } q = a \end{cases}$. This can be seen from the fact that since there are two constraints $f_1(q) = q - a \geq 0$ and $f_2(q) = b - q \geq 0$, one gets $\nabla f_1(a) = 1$, $\nabla f_2(b) = -1$.

A solution $q(\cdot)$ to $\mathscr{P}_F$ is shown to exist by studying the limit of the solutions of a sequence of approximating problems $\mathscr{P}_{n,F}$ with penalizing function $F_n(q_n, \dot{q}_n) = F_{n,1}(q_n, \dot{q}_n) + F_{n,2}(q_n)$ using Yosida's approximants for the elastic term, and a discontinuous function for the viscous friction term (such discontinuity is easily understandable looking at the example above: the total vector field of the system considering both contact and noncontact phases is continuous if only elastic terms are present, but it is not if viscous friction is added). It is worth noting that the viscous friction term contains a coefficient ε that is equal to $\frac{f}{2\sqrt{k}}$ in the preceding section on approximation when $0 < e_{\mathrm{n}} \leq 1$, see (2.9). It is easy to show that $\mathscr{P}_{n,F}$ reduces to our example in the particular one-dimensional case, although the meaning of the approximants in higher dimensions is not obvious. Let us illustrate the theory developed in [969] on this simple one degree-of-freedom case.

Example 2.2 [969] In the case when $n = 1$, $F \equiv 0$ and $\Phi = \mathbb{R}^+$, the system can be written as

$$\begin{cases} \ddot{q}(t) + \partial\psi_{\mathbb{R}^+}(q(t)) \ni 0 \\ \\ \dot{q}(t_k^+) = -e_{\mathrm{n}}\dot{q}(t_k^-) \qquad \text{for all } t_k \text{ such that } \; q(t_k) = 0, \dot{q}(t_k^-) < 0. \end{cases} \tag{2.39}$$

This is the dynamical equations of a point striking an horizontal obstacle, with no external forces. The approximating problem chosen in [969] is

$$\ddot{q}_n(t) + 2\varepsilon\sqrt{k_n}\dot{q}_n(t)\mathrm{sgn}^-(q_n(t)) + k_n q_n(t)\mathrm{sgn}^-(q_n(t)) = 0 \tag{2.40}$$

where $k_n \to +\infty$ as $n \to +\infty$, $\mathrm{sgn}^-(q_n) = \begin{cases} 0 \text{ if } q \geq 0 \\ 1 \text{ otherwise} \end{cases}$, and $\varepsilon = -\frac{\ln(e_{\mathrm{n}})}{\sqrt{\pi^2+\ln^2(e_{\mathrm{n}})}}$.[28] The quantity $e_{\mathrm{n}} \in (0, 1]$ is the restitution coefficient. Note that the function $\mathrm{sgn}^-(q_n)$ allows to write contact and noncontact dynamics in a single equation. The switching conditions are therefore chosen when the position vanishes (as we know this may yield negative reaction forces). The signs are reversed with respect to the examples we have treated above, since free motion occurs now for $q \geq 0$. The initial conditions are chosen as $q_n(0) = a > 0$ and $\dot{q}_n(0) = b < 0$. Hence the mass point starts in the free-motion space with a velocity directed towards the obstacle. Denoting $\tau = -\frac{a}{b}$ and $\tau_n = \tau + \frac{\pi}{\sqrt{k_n(1-\varepsilon^2)}}$, the solutions can be explicitly obtained and are (we recall them for convenience although they have been already obtained above):

$$q_n(t) = \begin{cases} a + bt & \text{for } t \in [0, \tau] \\ e_{\mathrm{n}}^{-\varepsilon(t-\tau)\sqrt{k}} \sin\left[(t-\tau)\sqrt{k(1-\varepsilon^2)}\right] \frac{b}{\sqrt{k(1-\varepsilon^2)}} & \text{for } t \in [\tau, \tau_n] \\ -\exp\left(-\frac{\pi\varepsilon}{\sqrt{1-\varepsilon^2}}\right) b(t-\tau_n) & \text{for } t \in [\tau_n, +\infty[\end{cases} \tag{2.41}$$

Then clearly $q_n(t)$ in (2.41) converges towards

$$q(t) = \begin{cases} a + bt & \text{for } t \in [0, \tau] \\ -e_{\mathrm{n}} b(t-\tau) & \text{for } t \in [\tau, +\infty], \end{cases} \tag{2.42}$$

whose derivative possesses a discontinuity at $t = \tau$.

In case when there is some external force acting on the particle in the Example 2.2, then in general the equations are not integrable. But [969, Theorem 2] guarantees that the solution set of problem $\mathscr{P}_F$ possess an element (not necessarily unique) whose first derivative is of bounded variation. The theorem is stated as follows:

Theorem 2.1 (Constant mass matrix [969]) *Consider the system defined in Problem 2.2. This system admits a solution in the sense defined as in Problem 2.2,* **a**, **b**, **c**, **d**.

[28] Compare the value of the damping in this sequence of approximating problems with the value of the damping in (2.9). It is a common calculation to compute e_{n} for the spring-dashpot model, see [175, Eq. (3.44)].

This solution is obtained as the strong limit in $W^{1,p}([0,T],\mathbb{R}^n)$ *for all* $p \in [1,+\infty)$, *and weak* $\star$ *limit in* $W^{1,\infty}([0,T],\mathbb{R}^n)$,[29] *when* $n \to +\infty$, *of a subsequence of the sequence of solutions of*

$$\ddot{q}_n(t) + 2\varepsilon\sqrt{k_n}G(q_n(t) - P_\Phi(q_n(t)), \dot{q}_n(t)) + k_n(q_n(t) - P_\Phi(q_n(t))) = f(t, q_n(t), \dot{q}_n(t)) \tag{2.43}$$

with $q_n(0) = q_{n,0}$, $\dot{q}_n(0) = \dot{q}_{n,0}$. $P_\Phi(\cdot)$ *denotes the projection on* Φ,[30] *and* $G(v,w) = \begin{cases} \frac{(v^T w)v}{v^T v} & \text{if } v \neq 0 \\ 0 & \text{if } v = 0. \end{cases}$

From the one-degree-of-freedom case in Example 2.2, the different terms of the approximating problems correspond to spring and damper-like actions, with the "usual" switching conditions of Sect. 2.1.3.1. It is clear that due to the chosen switching conditions, the damping term in (2.43) may induce discontinuities in the ODE right-hand side. One may choose to embed (2.43) into Filippov's framework of differential inclusions by convexifying the discontinuous vector field, hence guaranteeing the existence of global absolutely continuous solutions $(q_n(\cdot), \dot{q}_n(\cdot))$ (and, due to the particular structure of a mechanical system, $q_n(\cdot)$ is even continuously differentiable). The proof is redone from scratch in [969].

The proof proceeds in showing that $\mathscr{P}_{n,F}$ possesses L_∞-bounded solutions that converge to q, and that $F_{n,1}(q_n, \dot{q}_n)$ and $F_{n,2}(q_n)$ converge weakly$\star$ towards measures P_1 and P_2 such that $\ddot{q} - F = P_1 + P_2$, and (**c**) is true. The last part of the proof is dedicated to study the rebound conditions. It is clear that since this study encompasses the case of the bouncing ball with $0 < e_n < 1$, finite accumulation points in the impact sequence $\mathscr{P}_F$ are tolerated. This is in contrast with the results in Problems 2.1 and 3.1 that rely on energy preservation at impacts (see [260, Theorems 3 and 4] [989 Lemma 2.1], where it clearly appears that $t_k < t_{k+1}$ for all k is a crucial property for uniqueness). Theorem 2.1 may also be used to study the existence of solutions for the cable system dynamics in Example 1.6 when a restitution impact law is considered.

In Problem 2.2 and Theorem 2.1, the inertia matrix is supposed to be identity, so that the gradient on the configuration manifold is the one in $\mathbb{R}^n$, and the configuration space is Euclidean. On the other hand, the admissible domain Φ defined by the unilateral constraint may not be convex as supposed in Problem 2.2. Actually the convexity of Φ is convenient to assure a unique projection $P_\Phi(q_n)$ in the penalization. Some ideas allowing one to relax the convexity are given in [972, 973]. They are based

---

[29] $W^{1,p}$, $1 \leq p \leq \infty$, denotes Sobolev spaces [191].

Definition 2.2 Let $1 \leq p \leq +\infty$. The Sobolev space $W^{1,p}(I)$, where $I \subset \mathbb{R}$ is an open interval (bounded or not), is the set of functions $f(\cdot)$ such that

(i) $f \in L^p(I)$.

(ii) There exists a function $g \in L^p(I)$ such that $\int_I f\dot{\varphi} = -\int_I g\varphi$ for all $\varphi \in \mathscr{D}$ whose support is contained in I.

Any function $f \in L_p$ possesses a distributional derivative that belongs to $\mathscr{D}^\star$ (see definitions in Appendices A.1 and A.2). Then $f \in W^{1,p}$ if this distributional -or generalized- derivative coincides in $\mathscr{D}^\star$ with a function in L_p. See also Sect. A.1.3 for basic facts about strong and weak$\star$ convergence.

[30] This why Φ is assumed to be convex: this secures a unique projection.

on the use of a discretization of the dynamics, see Sect. 5.7.3. Schatzman relaxed both assumptions in [1070], using the kinetic metric to define the restitution rule in a specific transformed generalized velocity.[31] In [1070] the projection is however applied to positions, in order to enable one to formulate a penalized problem (i.e., a sort of generalized spring-dashpot).

Problem 2.3 (Non-Trivial Mass Matrix [1070]) Let the constrained dynamics be $M(t,q)\ddot{q} = F(t,q,\dot{q}) + \lambda$, where: $M(t,q)$ is twice differentiable, $F(\cdot)$ is continuous in all its arguments, locally Lipschitz continuous in q and $\dot{q}$. The admissible domain $\Phi \subseteq [0,T] \times \mathbb{R}^n$, its boundary $\mathrm{bd}(\Phi(t))$ is a submanifold of class C^3 of $[0,T] \times \mathbb{R}^n$. The vector valued measure λ and the position q satisfy:

- $q(t) \in \Phi$ for all $t \in [0,T]$,
- $\mathrm{supp}(\lambda) \subset \{t \in [0,T] | q(t) \in \mathrm{bd}(\Phi(t))\}$,
- $\lambda = \tilde{\lambda} M(\cdot,q) m(\cdot,q)$, where is the unitary exterior normal vector to $\Phi(t)$.

The vector $m(t,q)$ satisfies $m(t,q)^T M(t,q) m(t,q) = 1$, and when contact is active it is the normal to $\mathrm{bd}(\Phi(t))$ in the kinetic metric (which we shall denote as $\mathbf{n}_q$ in Chap. 6). In case Φ is finitely represented as $\Phi = \{q \in \mathbb{R}^n | f(q) \geq 0\}$, $f : \mathbb{R}^n \to \mathbb{R}$, then it is equal to $\frac{M(q)^1 \nabla f(q)}{\sqrt{\nabla f(q)^T M(q)^{-1} \nabla f(q)}}$ on its boundary. Imposing C^3 regularity on the boundary $\mathrm{bd}(\Phi)$ allows one to locally linearize it. The restitution law is applied to the velocity $\dot{q}_{\mathrm{n}} \stackrel{\Delta}{=} m(\cdot,q) \frac{d}{dt}[m(\cdot,q)^T M(\cdot,q)(q - P_{\mathrm{bd}(\Phi)}(\cdot,q))]$, where $P_{\mathrm{bd}(\Phi)}(\cdot,q)$ is the projection of q on the (time-varying) boundary. A generalized penalization term is introduced and the sequence of solutions of the penalized problems is shown to converge to solutions of the rigid body problem (uniformly for positions, strongly in all spaces L^p with $1 \leq p < +\infty$ for velocities).

Theorem 2.1 might also be considered as a mathematical preliminary study for dynamical analysis of systems like particles bouncing inside a closed[32] curve which are called in mathematical physics *billiards* [137, 683, 1114]. Thus the problem is completely treated from the existence of solutions (but not uniqueness) to the trajectories global behavior. It is noteworthy that the case of nonsmooth $\mathrm{bd}(\Phi)$ is treated also in [966], when the kinetic energy loss satisfies $T_L(t_k) = 0$ at impact times t_k. The shock conditions are then stated simply from the energy conservation equation (see Problems 2.1 and 3.1), which avoids the difficulty encountered with restitution rules at singularities, where the normal to the boundary $\mathrm{bd}(\Phi)$ at q does not reduce to a half-line in $\mathbb{R}^n$, but is the normal cone $N_\Phi(q)$. This proves the existence of a solution in the sense of Problem 2.2, with $\dot{q} \in RCLBV$, for billiards with nonsmooth boundaries and elastic collisions (inside a polygon for instance, see [683, §6.4]).

[31] The use of the kinetic metric to analyze impact dynamics in Lagrangian systems, may be traced back to [581, 589, 683], and in the first edition of this book [202]. It has been deeply used in [209, 210, 228].

[32] Note that closed is to be taken here in the physical or real-world meaning, whereas closed in the Paoli-Schatzman's problem is to be taken in the topological sense, i.e., the whole space itself is in fact closed.

The results of Paoli and Schatzman extend the results in [683, Chap. 1, Theorems 1, 2, 3 and 4] which possess a local-in-time nature only (they are based on singular perturbation like analysis). Schatzman's pioneering work in [1066] treated the same problem, but with an energy conservation equality. It is based on the use of Moreau-Yosida regularization arguments (intuitively, this consists of introducing some penalization into the contact model, see Appendix B).

2.4.3 Uniqueness of Solutions

Since the preceding results deal with the existence of solutions, it is natural to say few words on an other important property: the uniqueness of solutions. We will come back later on this in Chap. 5, in particular Theorem 5.3 states general conditions on the well-posedness of frictionless complementarity Lagrangian systems. In the following we illustrate through an example given by Aldo Bressan in [186], improved later in [80, 1066], how the external action on the system may imply non uniqueness of solutions.

2.4.3.1 Aldo Bressan's Counter-Example

We describe in this section a counter-example invented by Aldo Bressan [186] to prove that the addition of unilateral constraints can, even in very simple cases, yield nonuniqueness of solutions for some initial data, even if smooth (infinitely differentiable) forces are considered. Similar counter-examples have been derived and improved later in [80, 260, 1066]. Let us consider the one degree-of-freedom system:

$$\ddot{q}(t) = Q(t), \quad q(t) \geq 0 \text{ for all } t \geq 0, \quad \dot{q}(t_k^+) = -e_{\mathrm{n}}\dot{q}(t_k^-), \; q(t_k) = 0, \; \dot{q}(t_k^-) < 0, \tag{2.44}$$

and the function:

$$\varphi(t) = \begin{cases} 0 & \text{if } t \leq 0 \text{ or } t = \frac{1}{2^m} \\ \frac{1}{2^{nm}} f\left[2^m f(t - \frac{1}{2^m})\right] = \frac{1}{2^{nm}} f(2^m t - 1) & \text{if } \frac{1}{2^m} < t < \frac{1}{2^{m-1}} \\ g(t) & \text{if } t \geq 1, \end{cases} \tag{2.45}$$

where $m \in \mathbb{N}$, $n \in \mathbb{N}$. The functions $f(\cdot)$ and $g(\cdot)$ satisfy the following conditions:

$$\begin{cases} f : [0,1] \to \mathbb{R} & f(t) > 0, f(0) = f(1) = 0 \\ \frac{df}{dt}(0) = -e_n 2^{1-n} \frac{df}{dt}(1), \; n \geq 3, \; 0 < e_n \leq 1 \\ \frac{d^k f}{dt^k}(0) = \frac{1}{2^{n-k}} \frac{d^k f}{dt^k}(1), & k = 2, \cdots, n-1, \end{cases} \tag{2.46}$$

and:

$$\begin{cases} g(t) > 0 \ \text{ for } \ t \geq 1, \ g(1) = 0, \ \frac{dg}{dt}(1) = \frac{-e_n}{2^{n-1}} \frac{df}{dt}(1) > 0 \\ \\ \frac{d^k g}{dt^k}(1) = \frac{1}{2^{n-k}} \frac{d^k g}{dt^k}(1), \ k = 2, 3, \cdots, n. \end{cases} \tag{2.47}$$

Then the following is true:

Theorem 2.2 *[186] The functions $\varphi(t)$, $\ddot{\varphi}(t)$,$\cdots$, $\varphi^{(n)}(t)$ exist, are continuous and $\varphi(t) \geq 0$ for all $t \in \mathbb{R}$, $\varphi(t) > 0$ for $t > 0$ and $t \neq \frac{1}{2^m}$. The first derivative $\dot{\varphi}(t)$ exists, is continuous for all $t \neq \frac{1}{2^m}$ and*

$$\dot{\varphi}\left[\left(\frac{1}{2^m}\right)^+\right] = -e_n \dot{\varphi}\left[\left(\frac{1}{2^m}\right)^-\right]. \tag{2.48}$$

Hence one has defined a function $\varphi(\cdot)$ which is zero for negative times, then it is composed on $[0, 1]$ of the concatenation of arches whose length tend to zero when t tends to zero (with a sort of reversed accumulation point at $t = 0^+$, that one usually calls a *right-accumulation* because the impacts accumulate on the right of the accumulation time, here $t = 0$: the derivative $\dot{\varphi}(\cdot)$ starts with a reversed accumulation of jumps). Now assume that $\ddot{f}(t) < 0$ and that $\ddot{g}(t) \leq 0$. Then $\ddot{\varphi}(t) \leq 0$ for all $t \in \mathbb{R}$. Roughly, the idea is to get $q(t) \equiv \varphi(t)$ (hence $Q(t) \equiv \ddot{\varphi}(t)$), so that the mass bounces against the constraint (see (2.48)) with a restitution coefficient e_n. This can be obtained as proved in the following:

Theorem 2.3 *[186] Let us choose $Q(t) = \ddot{\varphi}(t)$ in (2.44). Then the functions $Q(t)$, $\dot{Q}(t)$, $\cdots$, $Q^{(n-3)}(t)$ are continuous. The trajectory $q(t) \equiv \varphi(t)$, $t \in \mathbb{R}$, possesses the initial conditions $q(0) = \dot{q}(0) = 0$ and satisfies $\dot{q}(t_m^+) = -e_n \dot{q}(t_m^-)$, $m \in \mathbb{N}$, i.e., it is a trajectory of the dynamical system in (2.44). The trivial trajectory $q(t) = 0$ for all $t \geq 0$ is also a solution of the dynamical equations in (2.44).*

Such a result is surprizing, since the applied force is always negative. Hence, if one initializes the system at rest on the surface $q = 0$, it should logically remain stuck on it. The underlying idea is to consider an external action $Q(t)$ which is negative, but such that its double integral $\varphi(t)$ is positive, is zero at $t = 0$, continuous, and with a first integral $\dot{\varphi}(t)$ that jumps when $\varphi(t)$ attains zero ($t_m = \frac{1}{2^m}$). Clearly such a function is not obvious to construct, but Theorem 2.2 guarantees its existence (an explicit construction of similar functions has been given for instance in [80, 260, 1066]). As shown in [80, 81] in a broader context admitting several frictionless unilateral constraints and a generalized Newton's restitution impact law, analytic data eliminate such right-accumulations of impacts.

2.4.3.2 Sufficient Conditions for Uniqueness

For the sake of completeness of the exposition of the existing mathematical studies on systems with unilateral constraints, we provide now the conditions that have been derived by some authors to prevent such nonuniqueness problems. Using a similar counter-example as [186], [260, 1066] show that uniqueness of solutions to $\mathscr{P}_Q$ may fail even for smooth Q, and give some sufficient conditions for uniqueness to hold:

Theorem 2.4 *[260] Let $Q(\cdot)$ be absolutely continuous in $[0, T]$, $Q \in L^1([0, T])$ and $Q(t) \geq 0$ for all $t \in [0, T]$. Then if $Q(0) > 0$ and $x(0) \neq 0$, $\dot{x}(0^+) \neq 0$, there exists a unique solution to the dynamical problem formulated as in Problem 2.1. If the initial conditions are admissible (i.e., if $x(0) = 0$ then $\dot{x}(0^+) \leq 0$) and if $\dot{x}(0^+)^2 - 2x(0)Q(0) > 0$, then the solution is unique also on $[0, T]$.*

Notice that the signs of the pre and post-impact velocities as well as those of the contact force, are reversed here because the constraint is written as $x \leq 0$ in Problem 2.1 (see Remark 1.4 in Sect. 1.3). The proof is based on several steps. The central fact is that there is a finite number of impact times t_k on $[0, T]$. A sufficient condition for this is that $\dot{x}(t_k^+)^2$ (or equivalently $\dot{x}(t_k^-)^2$) be strictly positive. The conditions of Theorem 2.4 aim at guaranteeing such condition, which can be verified using the conservation of energy equation. In another article [261] the same authors prove the following result:

Theorem 2.5 *[261] The uniqueness of solutions to the Cauchy Problem 2.1 is a generic*[33] *property in $Q \in L_1([0, T], \mathbb{R})$.*

This result shows the prevalence of problems $\mathscr{P}_Q$, i.e., in fact of a particular type of second order differential equations, with unique solutions, as it is the case for ODEs with continuous right-hand sides as Orlicz showed (see [1229]). Note that when the impact is lossless the simple dynamical problem studied in Chap. 1, Example 1.1, is a particular case of problem $\mathscr{P}_Q$ in [261] with a zero external action: thus the results in [261] on uniqueness of the solution trivially hold for that case. In [261] uniqueness is studied as follows: it is shown that for every solution $x(\cdot)$ to $\mathscr{P}_Q$ with force $Q \in L_1$, $Q(\cdot)$ simple[34] there is a sequence $Q_n(\cdot) \to Q(\cdot)$ in L_1 so that $\mathscr{P}_{Q_n}$ has a unique solution $q_n(\cdot) \to q(\cdot)$ uniformly in $[0, T]$. Roughly one then uses density of the set of simple and L_1-bounded functions in the set of L_1-bounded functions to obtain the result in Theorem 2.5.

The first result on uniqueness that applies to n-dimensional System has apparently been given by M. Schatzman in [1066], who established the following result, in addition to existence of solutions in a more general context (external forces are admitted). The problem is that of a system with constant (identity) mass matrix and no external forces, constrained in a convex set.

---

[33] See [533, p. 154]: a property is generic in E if the set G of elements of E which possess it, contains a dense (in E) open set. In a sense, one deduces from the property of density of a set in another one that there are elements of G "almost everywhere" in E.

[34] i.e., $Q([0, T])$ is finite, i.e., it consists of a finite set of numbers $c_1, \cdots, c_n$. In other words, the external action is piecewise-constant, with a finite number of values.

Theorem 2.6 *[1066] Consider the differential inclusion* $\ddot{q}(t) \in -\partial\psi_{\Phi}(q(t))$, $q(0) \in \Phi$, *where* Φ *is a closed convex set. If the boundary* $\mathrm{bd}(\Phi)$ *is of class* C^3 *and has strictly positive Gaussian curvature,*[35] *then the Cauchy problem admits a unique global solution (i.e., on* $[0, +\infty)$*) such that:* $q \in W^{1,\infty}([0, +\infty); \mathbb{R}^n)$, $q(t) \in \Phi$ *for all* $t \geq 0$, *the inclusion is satisfied in the sense of distributions,* $\dot{q}(\cdot)$ *has left and right limits everywhere, the energy is conserved. Moreover, if* $q(0) \in \mathrm{bd}(\Phi)$, *and* $\dot{q}(0^+)$ *is tangent to* $\mathrm{bd}(\Phi)$, *then* $q(\cdot)$ *runs along the geodesic of* $\mathrm{bd}(\Phi)$ *passing through* $q(0)$ *and tangent to* $\dot{q}(0^+)$, *with the speed* $||\dot{q}(0^+)||$. *If the initial data do not satisfy these constraints, then* $q(t)$ *is never tangent to* $\mathrm{bd}(\Phi)$ *and it has a finite number of reflections in a finite time.*

The considered system may be called a billiard. This result is extended in [989, 990] who prove uniqueness of solutions under some analycity conditions.

2.4.4 Further Existence and Uniqueness Results

Let us make a short bibliography of well-posedness results obtained in the literature, which do not necessarily rely on penalizing functions. The uniqueness problem has also been studied for a one degree-of-freedom case in [1069], see Chap. 1, Sect. 1.3.2. It applies to purely elastic as well as nonconservative collisions. A general uniqueness result is proved in [80] who shows that if all the data (including external actions) are piecewise analytical (which is not a restrictive assumption in most applications), then uniqueness of solutions holds and right-accumulations of impacts created by forces like in Bressan's counter-example (see Theorem 2.3) cannot occur: only left-accumulations of impact may exist [81, Proposition 4.11], like in the classical bouncing ball system. Multiple, orthogonal (in the kinetic metric) constraints as well as non conservative impacts are considered in [80]. A general well-posedness theorem is stated in Theorem 5.3 in Chap. 5, which summarizes various existence and uniqueness results obtained after the pioneering results by Schatzman [1066] and Monteiro Marques [866, 867]. Well-posedness problems can be attacked another way, using explicitly the so-called *complementarity conditions*. This is the essence of the studies in [517, 759, 1063, 1064], which essentially focus on Linear Complementarity Systems and are described elsewhere in the book. Other works may be situated in-between differential inclusions and complementarity systems [205, 212, 214, 215, 226, 438].

[35] Let a surface S in $\mathbb{R}^3$ be given by $q_3 = f(q_1, q_2)$, with $\frac{\partial f}{\partial q_1}(q_{10}, q_{20}) = \frac{\partial f}{\partial q_2}(q_{10}, q_{20}) \neq 0$ (these two vectors span the tangent plane to S at P) and the q_3-axis is normal to S at $P = (q_{10}, q_{20}, q_{30})$. Then the Gauss or total curvature of S at P is equal to the determinant of the Hessian of $f(q_1, q_2)$ at P, i.e., the matrix $\frac{\partial^2 f}{\partial q_1 \partial q_2} \in \mathbb{R}^{2\times 2}$. It is for instance easy to verify that a plane given by $q_3 = aq_1 + bq_2$ has zero total curvature at any of its points. The ideas generalize for higher dimensions.

2.5 Some Comments on Compliant Models

As announced in the introduction of this chapter, all the above results and models deal with one contact/impact point. The case of multiple contacts is much more tricky. Analysing the limit as the stiffness diverges, of a compliant contact model when several surfaces are hit at the same time, is a tough mathematical issue tackled in very few articles [973, 975]. As shown in [163] in the case of bilateral (equality) constraints with penalization, very complex phenomena may be found at the limit. A specific feature of unilateral constraints, is that if the boundary $\mathrm{bd}(\Phi)$ of the admissible domain Φ is not smooth (this is the case when multiple constraints are present), then $\mathrm{bd}(\Phi)$ cannot be transformed locally into a hyperplane with a diffeomorphism. However it is locally identifiable with its tangent cone $T_\Phi(q)$ at configuration q. As we shall see later in this book, the geometry of unilaterally constrained Lagrangian systems involves tangent and normal cones.

Penalization may also induce stiff differential equations. Usually, the characteristic time of a spring-dashpot model, is of order $\mathcal{O}(\frac{1}{\sqrt{k}})$. Some authors recommend to compute at least 1000 points during a collision. If k is of order 10^{10} Nm, this represents a collision duration of order 10^{-5} s, hence a time step $h \approx 10^{-8}$ s. Simulation may be quite time-consuming. Moreover the lack of continuity in the initial data, or nonuniqueness of solutions, that is the common situation with multiple rigid contacts, as well as unavoidable round-off numerical errors in contact detection algorithms, may indicate that quite complex and unpredictable behaviors may occur when penalizations are used. The limit solution usually depends significantly on how the limit is reached, as demonstrated by simple chains of aligned balls (see an example in Chap. 6, Sects. 6.1.1.1 and 6.1.3). Mechanically, this is related to the duration of impact (and the maximum compression times at each contact) that varies depending on the stiffness and influences the outcome. Let us end by mentioning a crucial issue related to the stabilization of the normal accelerations and contact forces during persistent contact phases: many numerical simulation results which are shown in the Multibody Systems literature, prove that compliant contact models may yield spurious oscillations which have no Mechanical meaning (as proved by comparisons with experimental data [401, Figs. 5, 6, 8, 11, 12]). The choice of the contact/impact model has to incorporate such drawbacks as well, and the designer (or the Control scientist) should have in mind that a good model is a model with a reliable, robust numerical integration method.

http://www.springer.com/978-3-319-28662-4

Nonsmooth Mechanics
Models, Dynamics and Control
Brogliato, B.
2016, XXI, 628 p. 107 illus. in color., Hardcover
ISBN: 978-3-319-28662-4